Aeronautical Research Institute, University of Tokyo
Report No. 346, July 1959

On the Aileron Buzz in the Transonic Flow

By

Haruo SAITO*

Summay. The fact that the flow pattern near the region of the shock-boundary layer interaction takes a certain finite delay time, which looks like depending mainly upon the thickness of the separated boundary layer induced by the shock wave, in adapting itself to the new steady flow pattern owing to the pressure impulses impinging on the region, is proved experimentally and it is pointed out that the delay time due to it is the main cause of the occurrence of the transonic aileron buzz and that the discussion of the phenomena on the basis of the go-and-return time for the pressure impulse with the sonic velocity between the shock and the aileron is inappropriate. It is also shown that the states of the aileron oscillation, which is neither convergent nor divergent, on a wing-aileron system under the same aerodynamic condition are always the same, that the angular velocities of aileron oscillation are inversely proportional to the square root of the aileron mass moment of inertia with the proportionality constant approximated by the square root of the aileron hinge moment coefficient in a steady-state flow, hence that the type of the oscillation is not a simple harmonic one, but a nonlinear oscillation with comparatively small terms associated with $\dot{\varphi}$. Moreover, the greater the frequency of an aileron attached to the same wing is, the smaller the amplitude becomes and their product is always constant. The statement made in the literatures that the effect of a spring attached to a wing-aileron system has no connection with the aileron-buzz characteristics is not the case, but, naturally, the higher the stiffness of a spring is, the higher the frequency and the smaller the amplitude are. With a special wing-aileron system devised so as to suck out the thick boundary layer developed on the wing surfaces, the aileron buzz phenomena could be eliminated, so it was shown that the effect of the thick boundary layer on the time lag is very large. Based on these experimental facts, the equation governing the character of the aileron oscillation is proposed, which is a nonlinear differential equation with a hinge moment term proportional to the angular velocity of the aileron cubed, and its rationality is given by the analysis of the data obtained in Reference [9]. Lastly the methods to prevent the aileron buzz are described, which are performed by decreasing the delay time through the suction of the boundary layer flow or by increasing the frequency through the reduction of the weight of the aileron and the attachment of a spring.

1. INTRODUCTION

For airplanes flying at transonic speeds, there appear many kinds of peculiar phenomena, the so-called "transonic abnormal phenomena", which are never experienced in low speed flight. For example, they are those of many kinds of trim changes, wing drop and aileron buzz, etc. Even among the phenomena about the aileron, there exist the variation of hinge moment characteristic, the reversal of aileron effectiveness and the aileron buzz, etc.

* Engineering Laboratory, Mitsubishi Electric Manufacturing Co., Ltd.

Above all, the phenomenon of aileron buzz is an entirely novel one, of which physical mechanism has not yet been explained decisively in detail in spite of many author's investigations. This phenomenon of aileron buzz was experienced at first without any precaution, and it was so severe that it damaged the aileron of the airplane. For the safety of the practical airplanes, it called for the attentions of many airplane designers and has been experimented upon by various investigators. As the result, it has been conjectured that the phenomenon of aileron buzz might be caused by the following reason: that is, with the appearance of the shock wave on the wing in the transonic speed range, the pressure wave caused by the deflection of the aileron, which is excited by certain disturbances in the flow field, takes a finite delay time to go and return between the shock wave and the aileron by certain causes, hence the aileron undergoes a kind of self-excited oscillation. Based on many literatures about this problem, the outline of characteristic of this phenomenon can be understood. However, those literatures can never reply to the essential question as to in what physical mechanism it occurs. Of course, they do not propose a method to predict the frequency and amplitude of the aileron oscillation which occurs on the aileron attached to a certain practical wing, and moreover, they do not give the method to prevent the aileron oscillation.

It is the purpose of this paper to study these essential problems further than ever and to clarify the physical mechasism of the phenomenon of the transonic aileron oscillation. In the first place, in Chapter 2, the results concerning the aileron buzz obtained in each reference are described briefly. Next, in Chapter 3, the manner of propagation of pressure waves is studied experimentally, because it is suggested from the results of Chapter 2 that it is most important to know whether or not the delay time, which is believed as the main cause of the transonic aileron buzz, has a longer time than the go-and-return time of the pressure wave with the sonic velocity. If it is so, it is important to know in what manner it propagates, especially in what form the separated boundary layer affects the delay time. In Chapter 4, the appropriateness of the go-and-return time with the sonic velocity for the explanation of the aileron buzz phenomena is discussed experimentally, namely, it is studied whether the frequency, for example, may be restricted by the reference frequency due to the go-and-return time with the sonic velocity. Moreover, the amplitudes and frequencies of the so-called transonic aileron oscillations without any restriction of aileron motion are experimented. As a result, it is found that the frequency of the aileron oscillation depends mainly on the moment of inertia of the aileron and a certain constant. In Chapter 5, the above result is rechecked by making use of the wing, which has the same wing section but a different size. Moreover, we see what kind of characteristic the constant has and how it can be contrasted with that of the steady-state flow. In Chapter 6, the absolute value of the constant is measured and it is shown whether or not it can be approximated by the hinge moment coefficient in the steady-state flow. In addition, the results obtained in Chapter 4 are checked again. If the occurrence of the phenomena of the aileron buzz studied

above is certainly due to a time lag and the development of the separated boundary layer induced by the shock is the main cause of it, the aileron oscillation may be eliminated in the ideal case with whole removal of the boundary layer flow. In Chapter 7, the possibility to prevent the aileron buzz through the removal of the boundary layer flow is examined and, in addition, the effect of spring upon the wing-aileron system is studied. In Chapter 8, on the basis of the above experimental results, it is discussed under what condition the aileron buzz occurs and how the aerodynamic and mechanical conditions determine the configuration of the aileron oscillation. Further, the methods to prevent the aileron buzz are discussed. Conclusions are described in Chapter 9.

2. Historical Survey

In America, the phenomena of aileron buzz were experienced already about 1945 parallel with the development of the high speed airplanes. Reference [*1*] is one of the reports at the first stage encountered with a standard RM-1 stability and control research pilotless aircraft. From the aerodynamical viewpoint, this standard RM-1 research model consists of a cylindrical body of fineness ratio 22.7 equipped with four cruciform wings and four cruciform fins. The wings and fins are swept back by 45° and are of constant chord NACA 65-010 airfoil section normal to the leading edge. The ailerons are attached to the tipside of the wing trailing edge and are 0.10 wing chord, 0.33 wing semispan and 100 percent mass-balanced. When the sustaining rocket was fired, the power supply to the aileron servomechanisms failed and, thereafter, the ailerons were free floating. According to the control position data, a violent high frequency oscillation occured on the aileron and wing. This oscillation was the phenomenon that came to be watched as the so-called "aileron buzz". Then the data showed that the wing and ailerons vibrated at a constant frequency for any given Mach number. Hence, it is supposed that this vibration may be a flutter as a combination of wing and ailerons. However, the frequencies of the vibrations recorded in the flight test were considerably higher than the wing structure frequencies measured. Hence, it was concluded that this vibration was not likely to be a sort of the conventional flutter. In order to determine the mechanical interrelation of the wing and aileron motions, in Reference [*2*], the natural frequencies of the wing in bending and torsion were changed by various method, but it had no apparent effect on the flutter even in the extreme case that the wing tip was fastened to a strut. On the other hand, with the aileron fixed, the wing did not flutter, so it was concluded that this aileron oscillation was of a new type which required only one degree of freedom of the mechanical motion. In Reference [*3*], the cambered wings such as NACA 23012, NACA 65-212 were tested in contrast to the symmetrical wing attached to RM-1 model in Reference [*1*], and it was proved that such cambered wings experienced the same aileron oscillation. In Reference [*4*], the aileron oscillation was found to occur irrespective of the variation of the sweepback angle between 0°～50°, and the Mach number at the onset of buzz was found to increase

with sweepback angle and to decrease with angle of attack for any sweepback angle. In addition, the curves of the lift coefficient with the Mach number for incipient aileron flutter for each sweepback angle are parallel to the lift-divergence curve of this airfoil section. Therefore, it is supposed that there is a close connection between the occurrence of aileron flutter and the appearance of shock wave on the wing. In Reference [5], the effects of the density of testing medium, of moment of inertia of aileron, of spring stiffness, of mass balancing, of angle of attack and of spanwise position of the aileron etc. were studied experimentally. As a result, the initial Mach number is relatively independent of the density, but there is a tendency for frequency to decrease with the decrease in density. In addition, under a constant-density condition, the aileron buzz frequency and amplitude increased with the increase in Mach number and the oscillation stopped abruptly as the shock position was on the rear of the aileron, indicating the buzz to occur in a limited range of Mach number. Moreover, small changes of aileron natural frequency had no appreciable effect on buzz characteristics. But there could be seen a tendency for buzz frequency to decrease with increasing aileron moment of inertia and the mass balancing had little effect on the frequency or initial Mach number of buzz. According to the results obtained in Reference [6], a flap, of which trailing edge thickness was the same with that at hinge axis, oscillated even at subcritical Mach numbers, and increasing the moment of inertia of aileron could not prevent buzz but could decrease the frequency considerably.

Putting the data obtained above together, the reason of the occurrence of the aileron buzz may be summarized as follows: after a shock appears on the wing, the pressure impulse caused by the deflection of aileron, which is excited by certain disturbances in the flow field, spreads into the circumference and is reflected back mainly from the shock to the aileron. The delay time during this motion of the pressure impulse may be finite differing from the case of low speed, and this delay time can be thought to make the oscillation system unstable. The simplest method to check this idea is to take a delay time required for the pressure impulse to go and return with the sonic velocity between the shock and the aileron. An empirical method of determining buzz frequencies, taking this delay time as a reference time, is presented in Reference [7]. The outline of this reference is as mentioned below. Inverting the go-and-return time for the pressure impulse, the frequency is written approximately as follows:

$$f_a = \frac{a(1-M)}{Kd},$$

where a is the mean velocity of sound between the shock wave and the aileron, M the mean Mach number, d the mean distance and K is a factor to account for any additional time. Then the phase difference of the pressure impulse to the deflection of aileron can be written as follows:

$$\phi = 360^\circ\left(1-\frac{f}{f_a}\right),$$

where f is the single-degree-of-freedom flutter frequency. Therefore, this oscillat-

ing system is subject to the aerodynamic force with the phase angle described above, the damping force and the spring force. On the contrary, the factor K can be determined empirically through the substitution of experimental data. As a result, it was shown that the value of K was about 4. And it can be shown that for the practical buzz frequency, $f_a > f > 0.5f_a$. But it is said that this statement is not always correct.

Then, as another reason, it is supposed that the shock-induced separation, which appears with the existence of a shock wave on the wing or the occurrence of the lift divergence, grows to some extent and this affects somewhat greatly. Moreover, if the oscillation simulating the phenomena of the transonic aileron buzz appears at a low speed on a wing-aileron system with separated flow, the importance of separated flow can be emphasized because of the nonexistence of shock waves and delay time to be required for pressure impulse. Based on these ideas, spoilers were used in Reference [8], and the flap and the spoiler were collaborated so as to protrude the spoiler upward as the flap deflects downward and this corresponded to the increase of the extent of separation. At first, a spoiler, which was flush with the wing surface as the flap was in 0 deflection, was used and this arrangement simulated an airfoil set at Mach number near $M_{\text{crit.}}$. But this model did not oscillate. Next, a spoiler which was made to protrude 1.7 percent chord on the wing surfaces as the flap was in 0 deflection was used and this arrangement simulated an airfoil with strong shock waves and the corresponding separated flow on the wing surfaces at Mach numbers above $M_{\text{crit.}}$. Tests revealed that with this model the flap oscillated continually. Lastly spoiler was cut off from the flap and was fixed rigidly to the airfoil with 1.7 percent protrusion on the wing surfaces, and the tests showed no oscillation. The second experiment revealed that the character of the oscillation of the flap with a wide spoiler was analogous to the transonic aileron buzz, and the first experiment corresponded to the fact that aileron buzz did not appear at Mach number near $M_{\text{crit.}}$ and it appeared only when the shock grew strong enough to separate the boundary layer extensively. The third experiment revealed that these oscillations could occur by coupling the motion of the flap and the separated flow, and not by the aileron buffeting due to the separated flow. Of course, it is far too hasty to conclude that these oscillations explain explicitly the transonic aileron buzz, but these tests at least demonstrate that the oscillation is analogous to the transonic aileron buzz, which occurs due to the separated boundary layer even in the absence of compressibility effect. Now, following the above statements, it is desired to acquire some information about the mechanism of the propagation of the pressure wave in the separated boundary layer flow. Reference [9] reported long time records of pressure by means of a flush-type electrical pressure cell at several points on the wing during the aileron buzz. The results show that the aileron motion is very nearly sinusoidal, while the individual pressures are periodic at the same frequency but are not sinusoidal. In addition, the hinge moment is small and the time lag is long as compared with those of the lower surface. Since the airfoil tested has a greater tendency toward separation on the

upper surface than on the lower surface, it may be concluded that the separation makes the hinge moment decrease and makes the delay time increase.

3. Experiment 1

3.1. *Preliminary Consideration*

As has been stated in Introduction, the purpose of the present work is to clarify the manner of propagation of pressure waves between the aileron and the shock wave. So it is most desirable that the manner of their propagation for the aileron displacement on a real airfoil, including the interaction between the upper and lower surfaces, should be known. But this is far from feasible with the size of the wind tunnel available. Moreover, it is supposed that the interaction between the upper and lower surfaces has little effect on the buzz frequency itself, and that it only acts to duplicate the buzz amplitude. We may consider one surface only, and need not to specify a particular airfoil. Thus, with the ease of construction also taken into account, a straight-walled nozzle was chosen to represent a pattern corresponding to the pressure distribution upon an airfoil.

3.2. *Model tunnel and Equipments*

Fig. 1 shows the sketch of the model tunnel. The wind tunnel is a small one 740 mm in total length, 400 mm in height, and 50 mm in inner-wall width. The

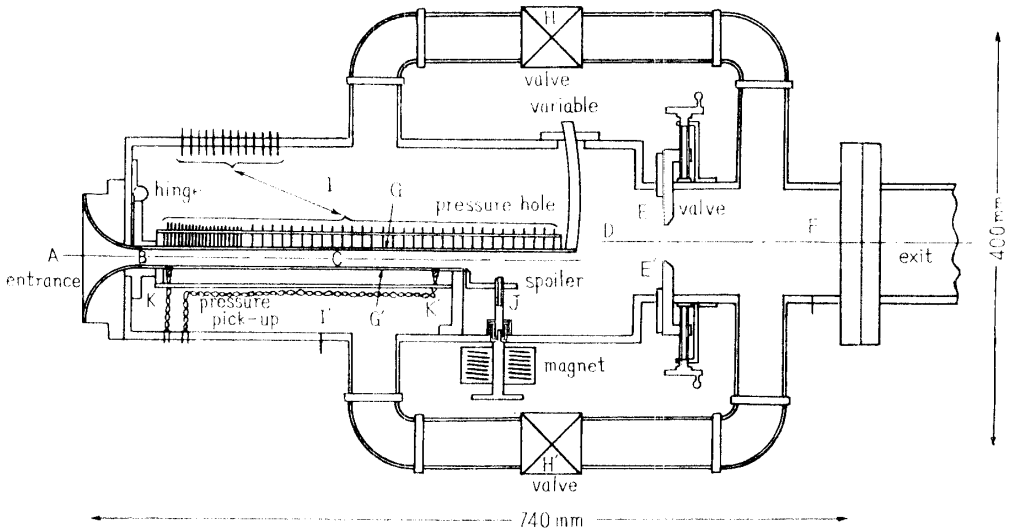

Figure 1. Transonic nozzle model (width 5 cm).

exit on the right of the figure is connected to the large vacuum tank in the 15th Building of the Aeronautical Research Institute, and the tunnel operates as a suction-type. The main flow passes from the entrance A, through the throat section B, to the nozzle C, and, after it has once entered the plenum chamber D, undergoes the mass-flow regulation by the collaborate valves E and E′, and then streams out into the low pressure part F. The upper and lower walls, G and G′ respectively, are slotted walls. G′ is fixed, while G is variable and can be set at

an appropriate angle. In order to approximate them to porous walls and, at the same time, to prevent the pressure waves from escaping directly through the slots, glass fibre was filled outside G and G′. Regulating the controlling valves H and H′, a fraction of the main flow was sucked out, through the slotted walls, into the external plenum chambers and then streams out into the low-pressure part F through the valves H and H′. A spoiler, which protrudes out perpendicularly into the flow by the action of a magnet, was placed on the fixed-wall side downstream of the channel, and two barium-titanate pressure pick-ups were attached on the inner surface of the fixed wall in order to measure the pressure propagation. Furthermore, a number of pressure holes to measure the pressure distribution of the steady flow were drilled on the variable wall, and some pressure holes are also present to measure the plenum chamber pressures in I, I′, D and the vacuum-side pressure respectively. The entrance section was made of wood, while the entrance cone attached to the variable wall was made of metal, as it moves with the variable slotted wall. The slotted walls are 50 mm in width and have five 1 mm-wide slots, so that their opening ratios are 10 percent. At first, the barium titanate was directly attached on the metal mould and inserted in these slotted walls. But this type of pressure pick-up proved to have poor sensitivity because of the pressures imposed from the sideward direction. Accordingly, a new type as shown in Fig. 2, which is insensitive to sideward pressures, was designed. Fig. 3 shows the sensitivity curve of this type of pick-up obtained from oscillograph

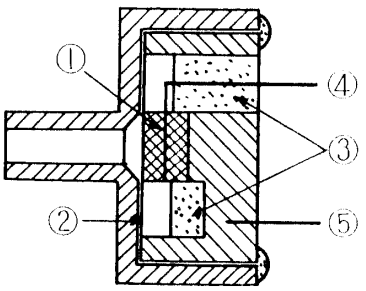

① barium titanate (2 plates)
dia. = 3 mm, width = 1 mm,
② silver foil,
③ material to adhere,
④ lead wire (+),
⑤ lead wire (−)

FIGURE 2. Pressure pick-up.

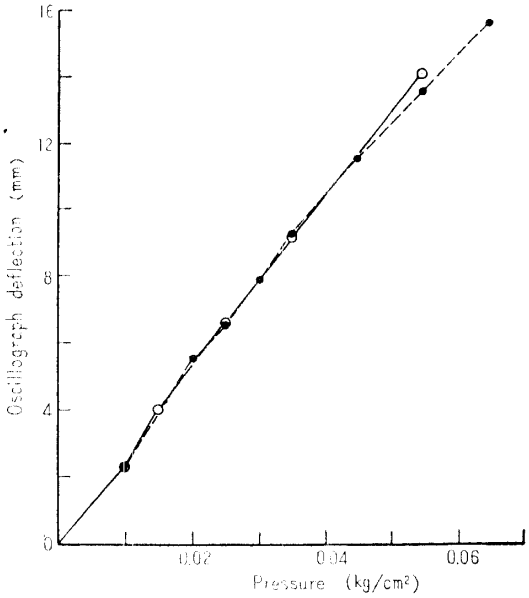

FIGURE 3. Sensitivity of pressure pick-up.

readings of its output, when the pressure pulses of known amplitudes were applied. Its characteristics may be regarded as almost linear. Two of this type of pressure pick-ups were placed at just upstream of the spoiler and near the throat, that is, practically just behind the shock, respectively, and their pressure waveforms are observed. Fig. 4 is the block diagram of the measuring circuits and details of the

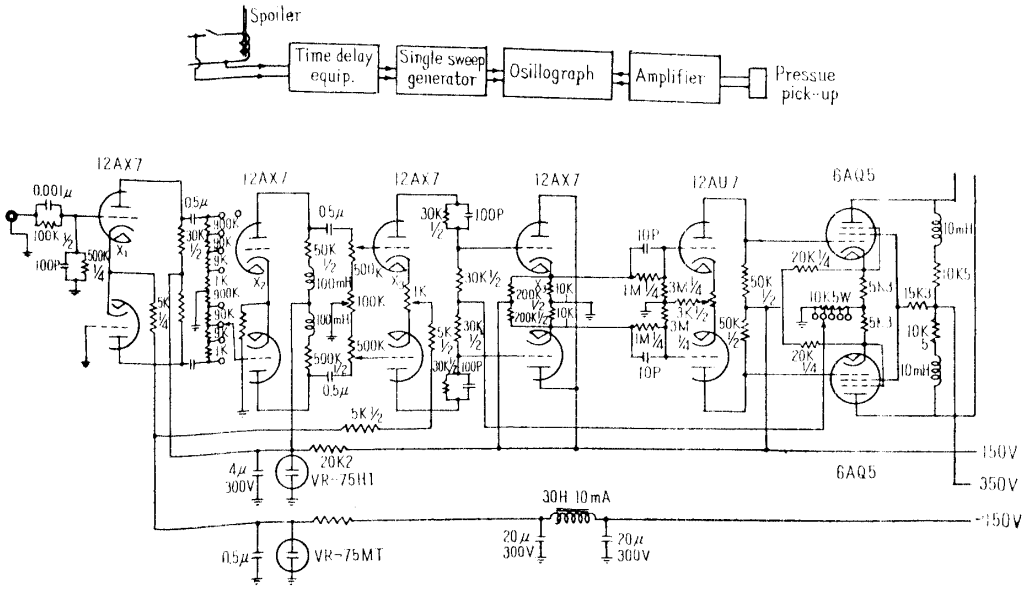

FIGURE 4. Circuit block diagram and amplifier detail.

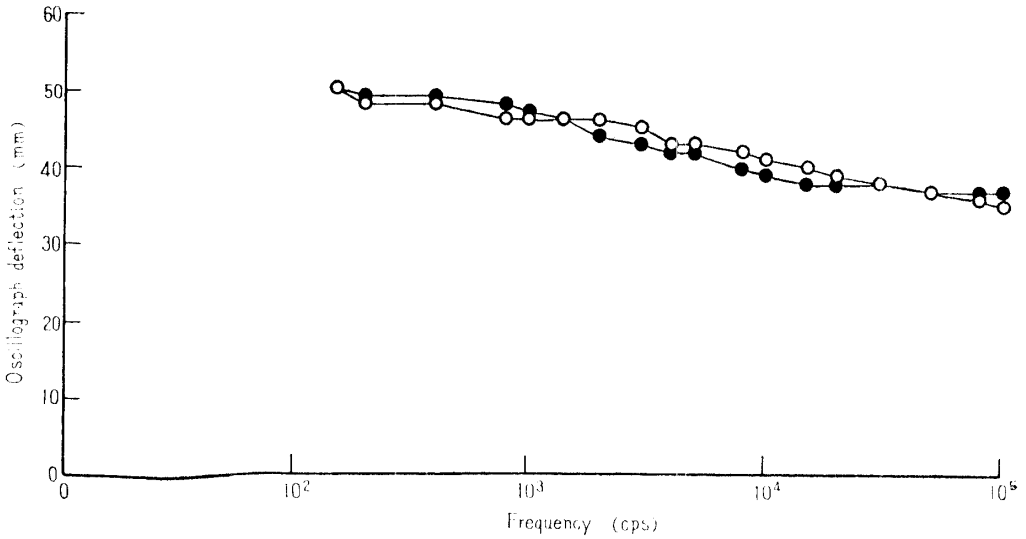

FIGURE 5. Frequency responce of pressure measuring equipment.

amplifier circuit. The oscillograph is a two-gun, single-sweep Braun-tube oscillograph. This was too expensive for our laboratory, but, fortunately, the author could borrow one from the Technical Research and Development Institute, Japan Defence Agency. The capacity of the barium titanate used as the pressure pick-up is about 170 pf. Its frequency response, when coupled with the measuring circuit, is shown in Fig. 5, and is satisfactory for the present experiment.

3.3. *Results and Discussion*

The outputs of the pick-up placed near the spoiler were recorded in the first place, since it is, above all, necessary to know how long it takes for the pressure pulse generated downstream to go and return, especially when the extent of the separated boundary layer induced by the shock changes. The variable wall was fixed at a certain angle, and the mass flow to be removed through the slotted walls was

controlled at an appropriate quantity with the valves. Under these conditions, the mass flow of the main flow was so controlled by the valves E and E′ as to locate the shock wave just before the pressure pick-up K. Then the spoiler was protruded by exciting the magnet, and the output of the pressure pick-up was fed to the Y-axis of the oscillograph, the single sweep being initiated by the signal that had passed through the delay circuit. As shown in Reference [*10*], the compression wave produced by the spoiler comes back as an expansion wave, after hitting the shock wave. Therefore, the waveform described by pressure pick-up K′ takes a shape shown in Plate 1. The location of the rise of the wave form corresponds to the time instant of the passage of the compression wave, and that of the fall to the time instant of the arrival of the expansion wave. The time

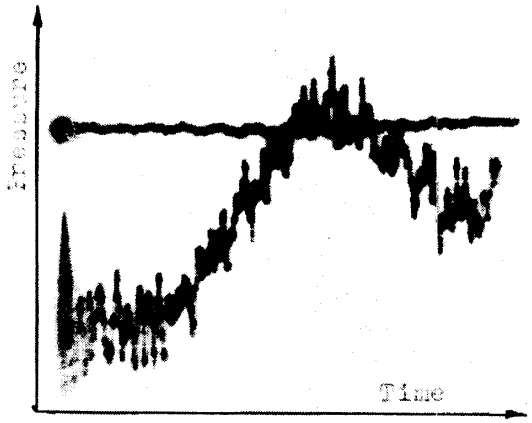

PLATE 1.

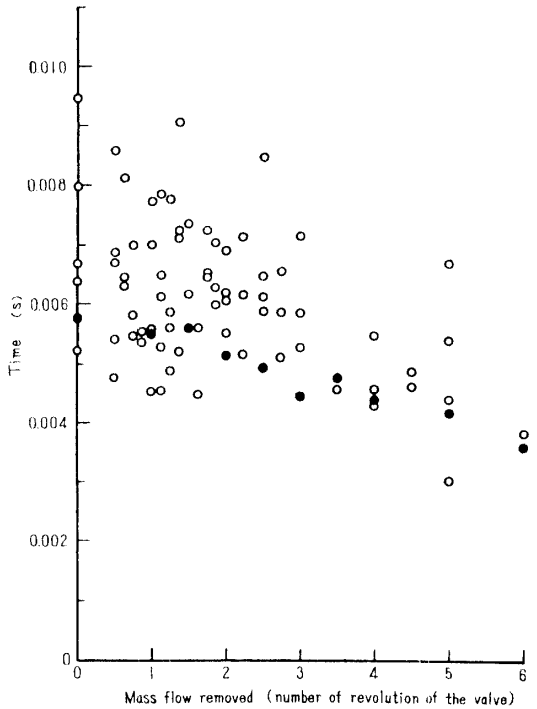

FIGURE 6. Delay time (wall opening 3°22′).

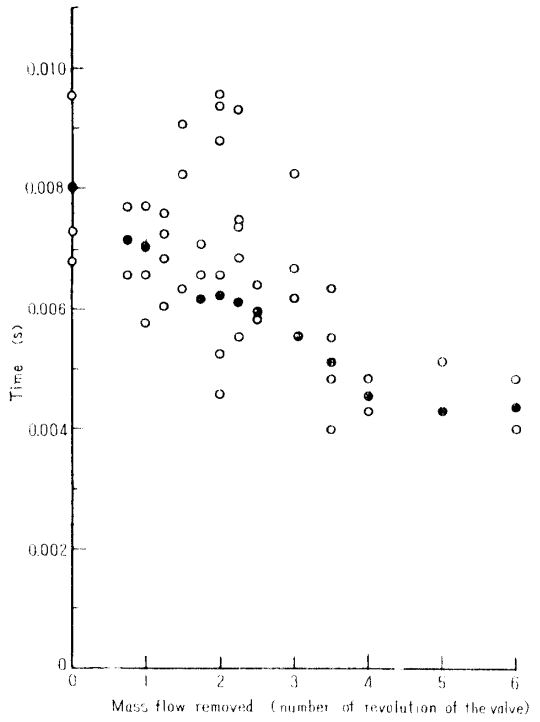

FIGURE 7. Delay time (wall opening 2°50′).

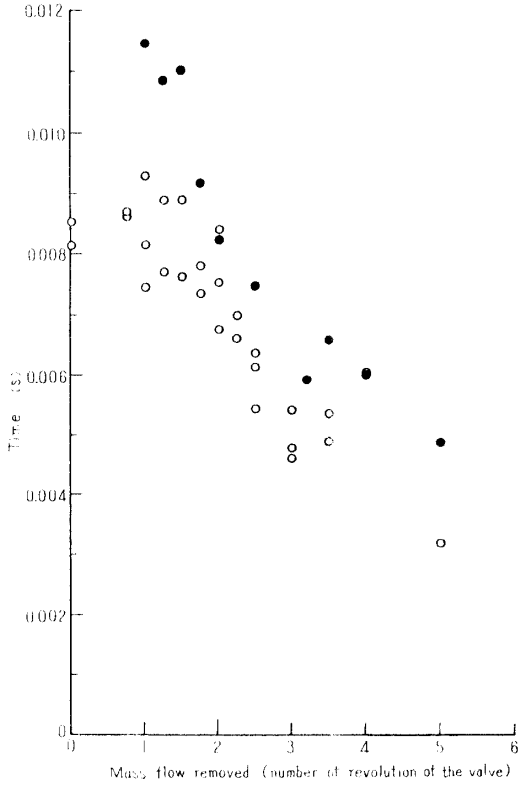

FIGURE 8. Delay time (wall opening 1°28′).

interval between them shows the go-and-return time of the pressure wave. In this experiment, the angle of divergence of the slotted walls were set at three values, 3°22′, 2°50′ and 1°28′, so that the situations might correspond to those on various airfoils, and the suction was changed from 0 to 6 revolutions in terms of the valve rotation. Figs. 6, 7 and 8 show the go-and-return time curves of pressure waves for various suction rates at the three opening angles of the slotted walls, respectively. The white circles in the figures are experimental points, while the black circles indicate the go-and-return times of sound waves calculated on the basis of the static pressures measured by the pressure holes on the variable wall. The approximate absolute values of the mass flow removed corresponding to each opening of the suction valve are calculated from the pressures in the plenum chambers I and I′, the pressure on the vacuum side F and the opening area of the valve, and they are shown in Fig. 9. In making a rough estimation of the mass flow in the boundary layer upon the slotted walls, the boundary layer in front of the shock is disregarded, and that behind the shock is assumed to be turbulent. The results are the straight lines in the figure, and it may be supposed that the suction rates are fairly sufficient. We see in Figs. 6 to 8 inclusive that the go-and-return time of a pressure wave is practically the same as that of the sound wave, if the experimental errors are taken into account. Besides, this holds whatever the suction rate may be. However, such a result is rather expected, and there is nothing so strange with it. It is rather supposed that the propagation of a pressure disturbance takes place in a manner that can be readily imagined, but

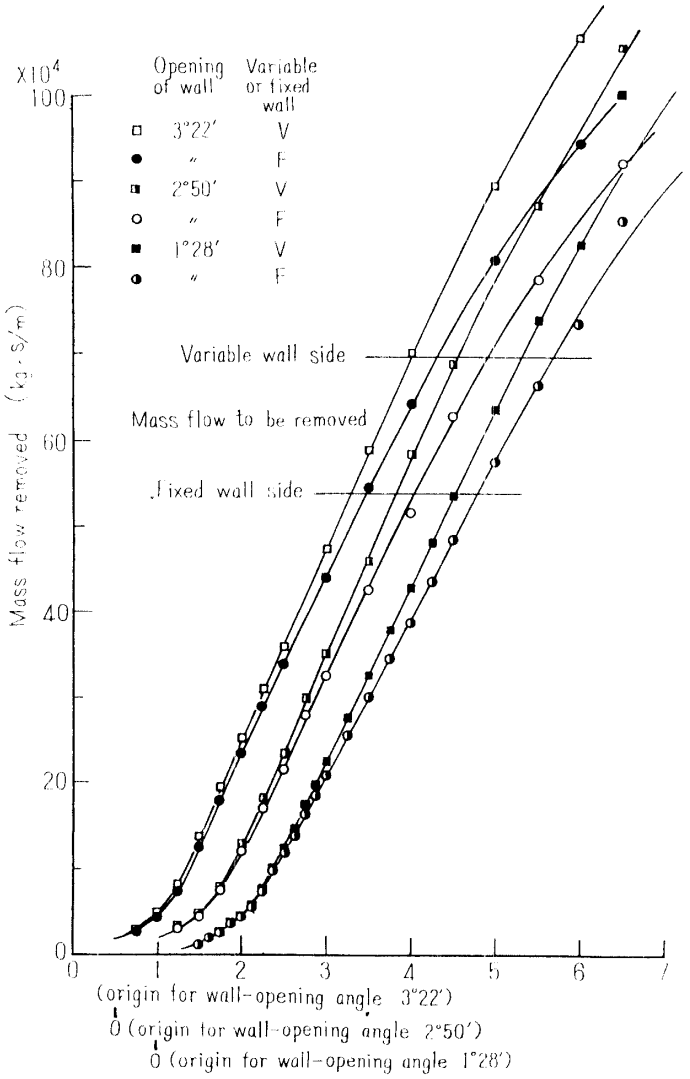

FIGURE 9. Mass flow removed.

that some delay time for the whole pressure change is brought about due to the occurrence of the shock-boundary layer interaction. Considering this fact, not only the go-and-return times but also the pressure variation history at a position

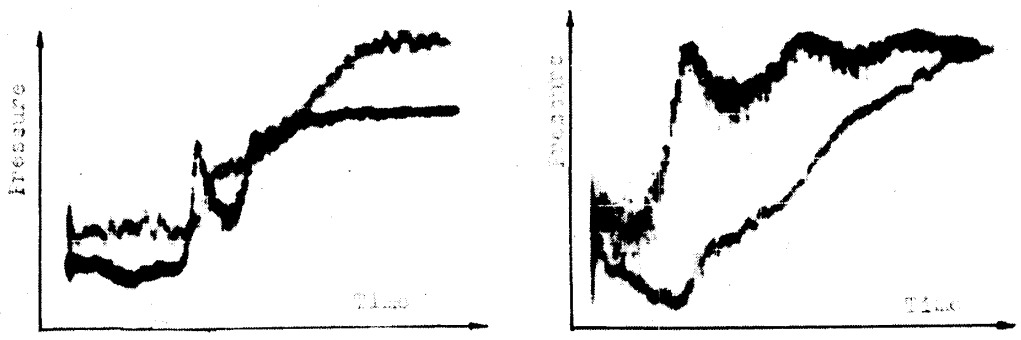

(a) (b)

PLATE 2.

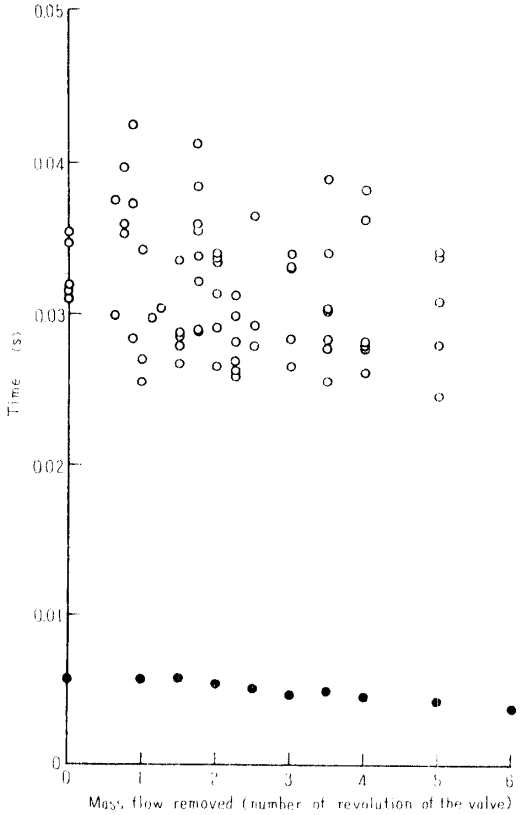

FIGURE 10. Delay time (wall opening 3°22′).

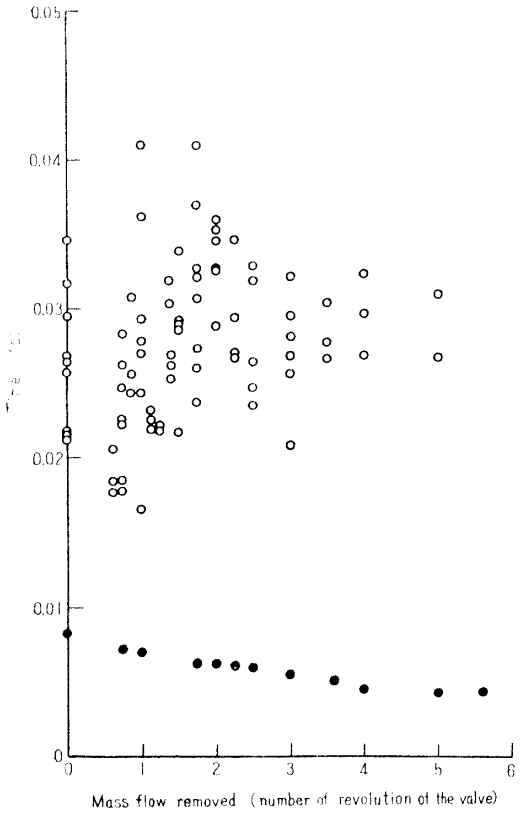

FIGURE 11. Delay time (wall opening 2°50′).

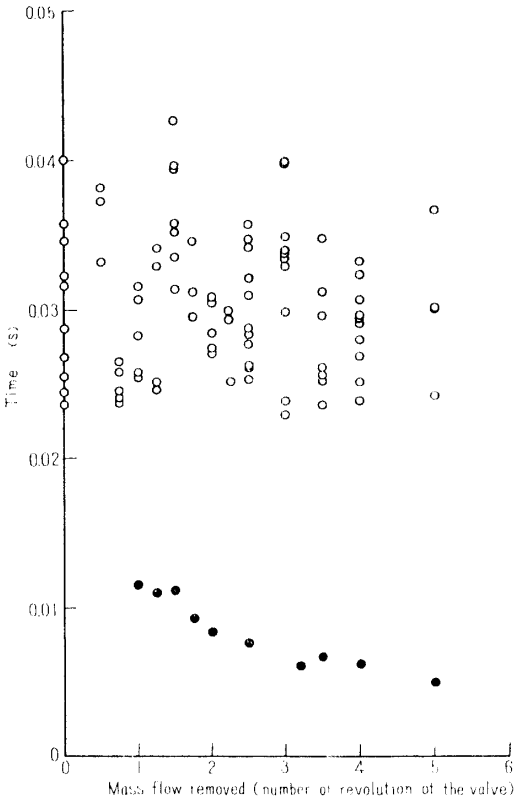

FIGURE 12. Delay time (wall opening 1°28′).

just behind the shock wave was recorded for a fairly long stretch of time. Plates 2(a), (b) show typical configurations in this case. The pressure just in front of the spoiler is hardly affected by the subsequent change in the flow, and merely oscillates due to the pressure change by the reflected wave, since the pick-up position is immersed in the dead-air region produced by the spoiler protrusion. Meanwhile, it is clearly seen that the pressure just behind the shock reaches a steady value after a fairly long time compared with the go-and-return time of the pressure wave. Therefore, it may be concluded that it takes a certain delay time for a a point in flow where the shock-boundary layer interaction is occurring to adapt itself to the new boundary condition corresponding to a pressure change. Besides, it is clearly seen from the photographs that the pressure changes linearly with time during the delay time. Figs. 10 to 12 inclusive show these delay times measured just as those of Figs. 6 to 8 inclusive. For various suction rates, the delay times are almost constant. In this experiment, it was difficult to locate the shock wave on the slotted wall, and it was located on the solid wall just upstream. Accordingly, the condition of the boundary layer at the shock wave position may have changed very little even when suction was operating. Thus, it may be remarked that these delay times are determined by the condition at the shock-boundary layer interaction point, and fairly unaffected by the conditions in halfway.

Next, the pattern of the pressure variation with time, when the heights of the protrusion of the spoiler were changed, was recorded in order to see how the delay time depends upon the magnitude of the pressure impulses. Plates 3(a), (b) are the

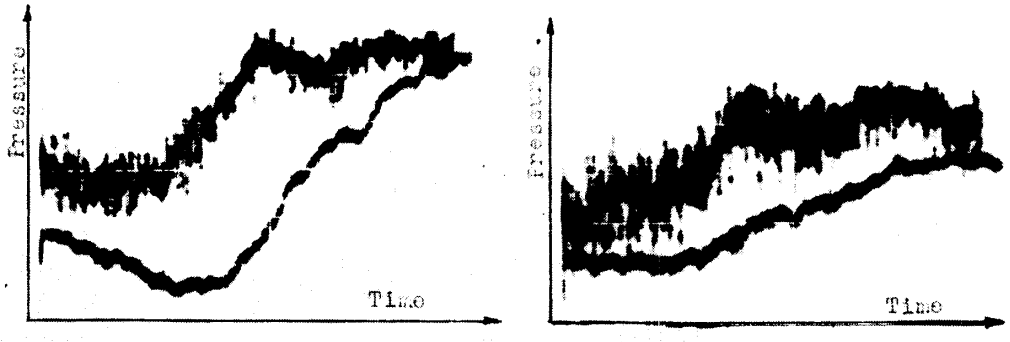

(a) (b)

PLATE 3.

typical examples and both of them correspond to the same opening of the nozzle 1°28′ and to the same opening of the suction valve 2. In addition, the scales of time and pressure for both pictures are equal but the heights of the protrusion of the spoiler are 7 mm and 4 mm respectively. We see in these photographs the facts that the larger the height of the protrusion is, the greater the corresponding pressure increment becomes, which is a matter of course, and that both time durations required to reach the steady state are nearly identical. This suggests that the delay time may be almost determined by means of the quantities associated

with viscosity such as the thickness of the boundary layer independently of the intensity of the pressure impulse or the travelling distance and the velocity of the shock movement. Therefore, if all the data obtained in many references fall on a curve in $t \sim \delta^2/\nu$ plane, it may be concluded that the time lag is certainly due to the development of the viscous layer and depends mainly upon the thickness of the boundary layer, provided t is the delay time between the aileron motion and the hinge moment to it during the actual aileron oscillation and δ is the thickness of the separated boundary layer induced by the shock and ν is the kinematic viscosity. Unfortunately, however, we have no data to be able to conjecture both t and δ at hand and it is only the datum from this experiment that is available. Plate 4 shows the flow pattern inside the nozzle near the throat of

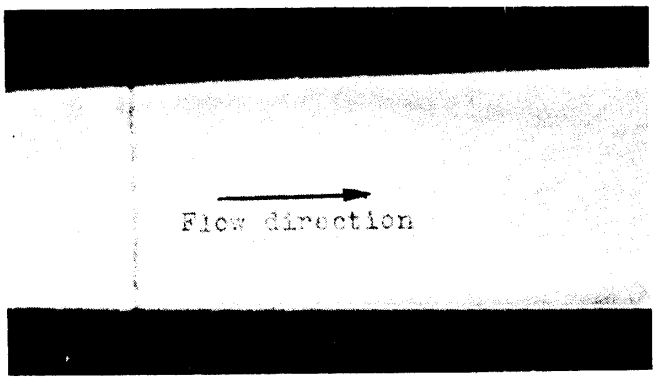

PLATE 4.

this case. The knife edge was set parallel to the flow direction, so the normal shock is obscure but it is near the thread stretched normal to the flow direction. As the height of the nozzle at the thread position is about 17 mm, the thickness δ of the boundary layer immediately after the normal shock can be measured as about 3 mm. On the other hand, if an infinite plane moves suddenly parallel to itself at a uniform velocity, the thickness of the fluid following the plate after the time t is about $5\sqrt{\nu t}$. According to this relation, the time interval corresponding to the measured thickness 3 mm is about 0.025 s. and this is the same order with the delay time 0.03 second obtained by the present experiment. It is far too hasty to conclude on the basis of this one datum that the delay time may be calculated similarly to the so-called Rayleigh's problem, but the delay time required for the boundary layer to adapt itself to the new state has probably a large effect on the appearance of the aileron buzz rather than the go-and-return time of the pressure wave with the sonic velocity outside the boundary layer, and the mechanism may be understood so as to make up or cancel the boundary layer with the same thickness in the region of the shock movement. The large effect of the boundary layer on the delay time can be emphasized also through the fact that the aileron oscillation stopped with the suction of the boundary layer flow, which will be described in Chapter 7. Therefore, it is concluded from these facts that the use of the go-and-return time of the pressure wave with the sonic velocity as a reference time is meaningless.

4. EXPERIMENT 2

4.1. *Preliminary Consideration*

According to the results acquired from the Experiment 1, it may be considered that the region of shock-boundary layer interaction takes a comparatively long time to adapt itself to the new boundary condition and that this is the main cause of the occurrence of the aileron buzz. While, if the reference frequency based on the go-and-return time of the pressure wave with the sonic velocity is valuable and additional factor is correct as was described in Introduction, the frequency of the aileron oscillation is expected between $0.5f_a$ and f_a. On the other hand, if it may be different, considering the facts in Chapter 2, it will mainly depend upon the moment of inertia, spring constant and the damper coefficient etc. However, the use of a spring or a damper is additive, so only the moment of inertia of the aileron is changed in this Chapter to prove experimentally whether the frequency of the aileron buzz depends only on the delay time stated above or not. Furthermore, the mass balancing of the aileron has been neglected, because it is believed that it has no effect on the oscillation itself. We have no systematic experimental data concerning the frequencies and the amplitudes of the aileron buzz at hand and have no clear information about them, hence the measurements about them are accentuated in this experiment.

4.2. *Model and Equipments*

The wind tunnel used in this experiment is a small suction-type transonic tunnel connected to the same vacuum tank as utilized in experiment 1. The test section is 40 mm × 94 mm in cross section, and the upper and lower walls are slotted walls with four 1 mm-wide slots on them resulting in a 10 precent opening ratio. The mass flow removed through the slots is absorbed into the low-pressure part which connects the plenum chamber to the tank. The Mach number is changed by regulating this mass flow removed with the valve fitted up near the low-pressure part. For low Mach numbers, the regulation is also made by changing the angle of the flap inserted in the hinder part of the parallel slotted walls. The Mach number is measured, as conventional, with reference to the plenum-chamber pressure. In order to eliminate the condensation effect in the wind tunnel, the

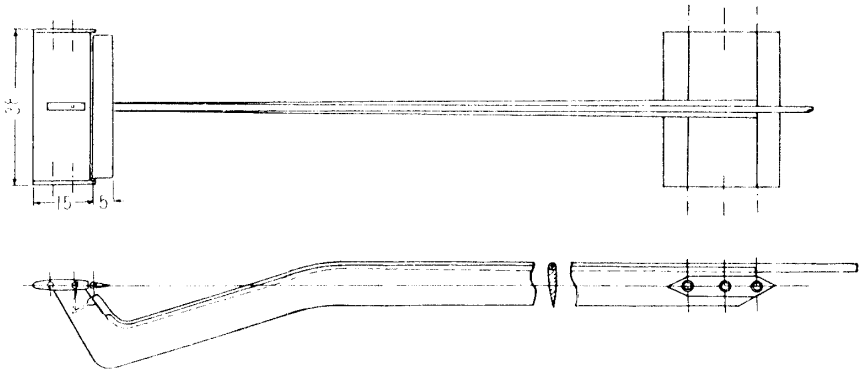

FIGURE 13. Model used in experiment 2.

air in-flowing from the atmosphere is passed once through the silica gel layers and effectively dried. Fig. 13 shows the model used here. The planform is a 40 mm × 20 mm rectangle and the section is 63_2A015. Since, generally, for a larger thickness, $M_{crit.}$ is lower so that a lower Mach number may be sufficient to bring the airfoil into the aileron buzz region, the 15 percent thickness was chosen. 63-series airfoil was chosen because of the conjecture that, the more distant the shock is located from the aileron, the longer the time lag and the lower the frequency become so that the oscillation may be the more ready to occur. It was attempted to make the boundary layer turbulent by cutting three stripes of grooves upon each surfane of the airfoil. The chord length of the aileron is 25 percent of the wing chord, its span is 36 mm, and the aileron itself is supported by means of a hinge rod inserted into the holes drilled on the plates, which, in turn, are attached to the both side of the wing. The wing and the strut were of mild steel, while three kinds of ailerons, one wholly of mild steel and the others of "hinoki" wood and of balsa, respectively, with the hinge rods only made of steel, were utilized. As our main concern was the buzz frequency and amplitude, the measurement consisted of phtographing, with a high-speed drum camera, the motion of the aileron while in buzz. The drum camera is made by Riken Keiki Co. Ltd., and the roter diameter is 242 mm. The rotor revolution rate can be adjusted from 0 to 2800 rpm, but it was fixed at 150 rpm throughout this experiment. The light source was a 500 V, 0.7 A water-cooled ultrahigh-voltage mercury lamp.

4.3. *Results and Discussion*

Plate 5(a), (b), (c) show the examples of the data obtained with the high-speed camera for the mild steel, "hinoki" wood and balsa ailerons, respectively. The oscillations of the mild steel and balsa ailerons were fairly regular, while the "hinoki" aileron oscillated rather irregularly. Besides, as it began to oscillate

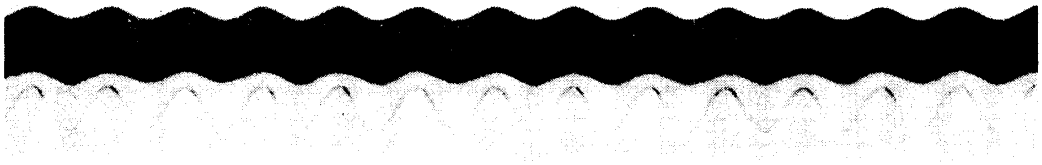

(a) Metal flap.

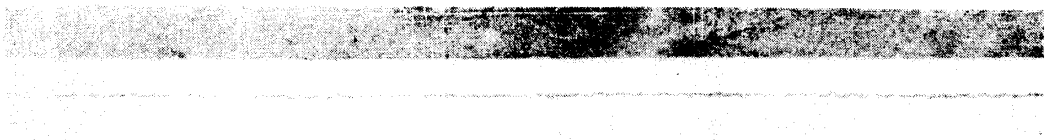

(b) "Hinoki" flap.

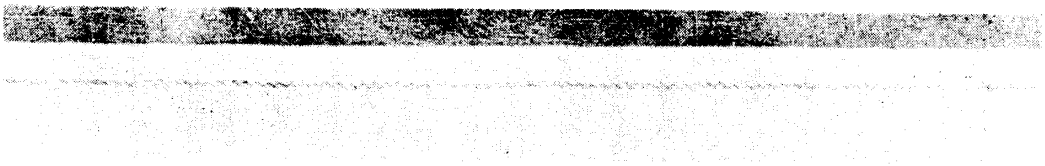

(c) Balsa flap.

PLATE 5.

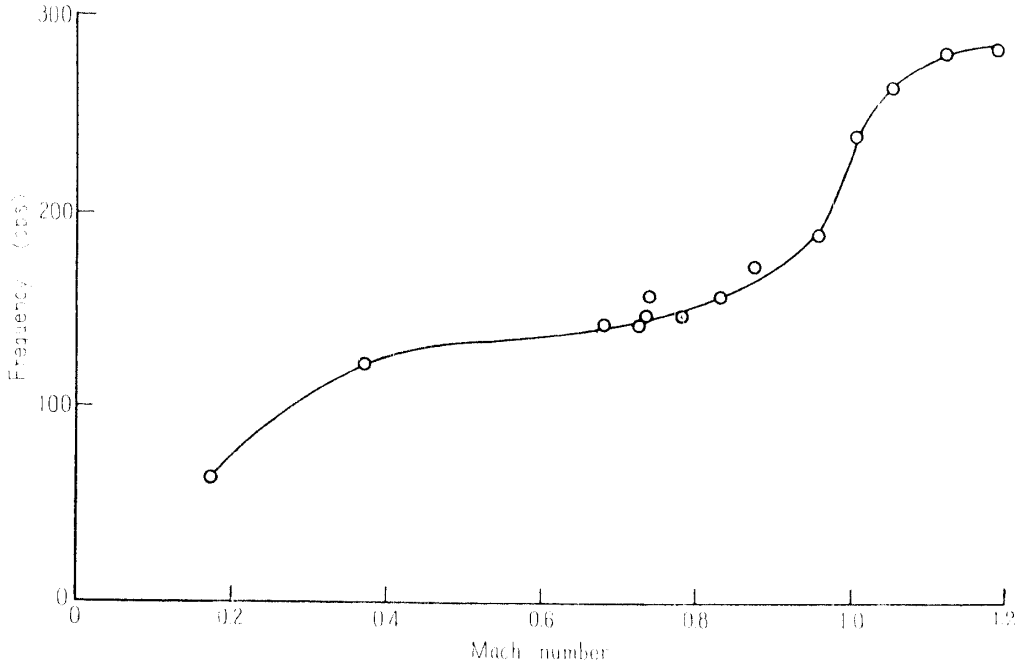

FIGURE 14. Buzz frequency versus Mach number (metal flap).

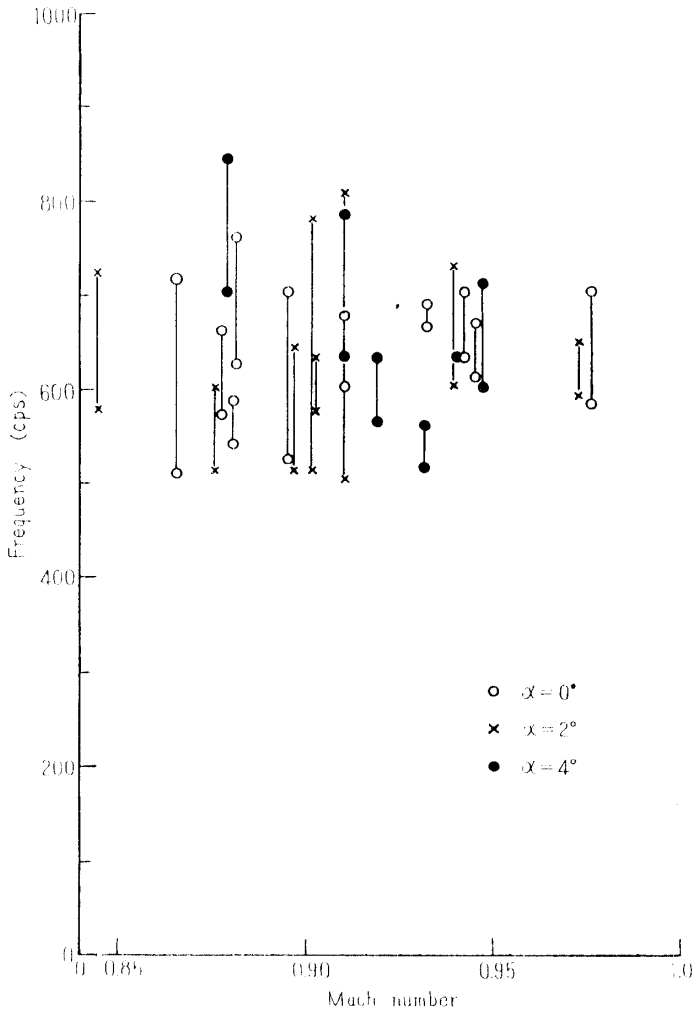

FIGURE 15. Buzz frequency versus Mach number ("hinoki" flap).

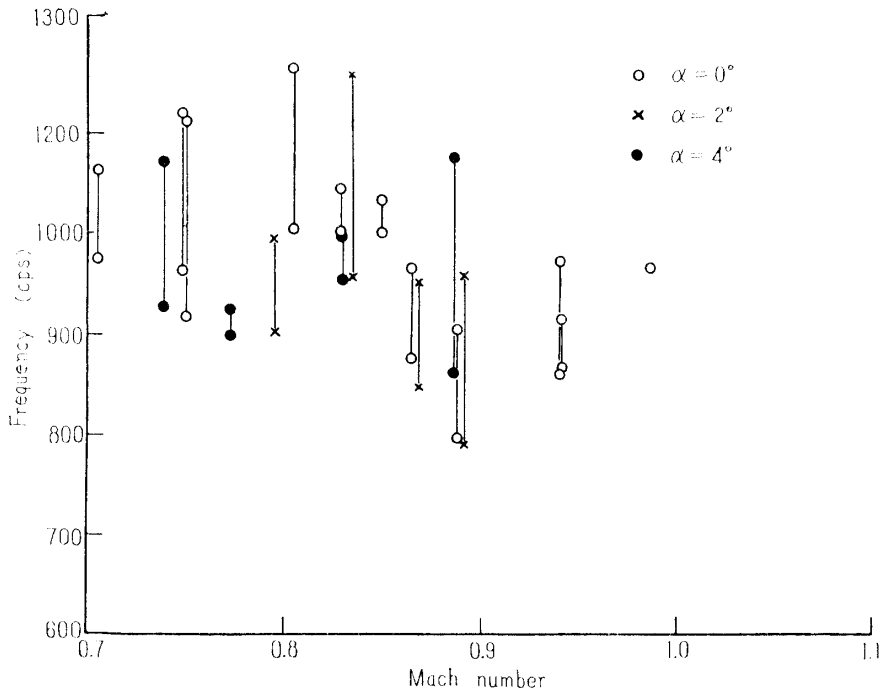

FIGURE 16. Buzz frequency versus Mach number (balsa flap).

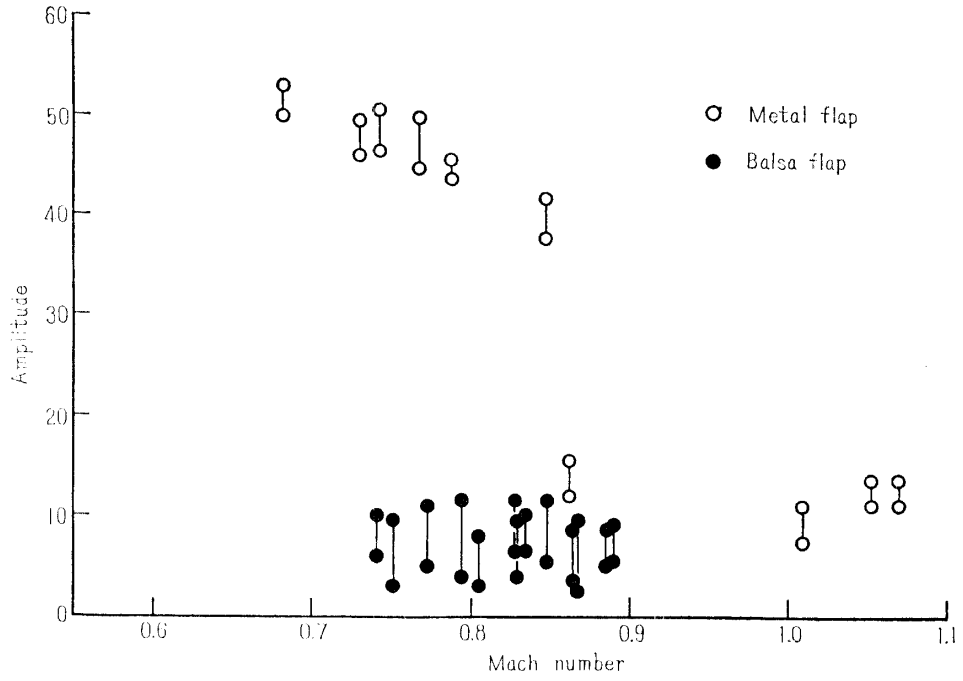

FIGURE 17. Buzz amplitude versus Mach number.

slightly only when the Mach number was very high, the data obtained for it were limited. In Figs. 14 to 16 inclusive are plotted the curves of frequency versus Mach number based on these data. Fig. 17 shows the amplitude curves. It was expected that the mild steel aileron would oscillate at the smallest amplitude because it had the largest moment of inertia. But the result was quite the contrary. As we see in Plate 5(a), its oscillation was very serious and the deflection

angle amounted to 75 degrees in total. Due to the intense oscillation, the airfoil itself, which was fixed on the strut, oscillated intensely with its environment, till it got broken and blown away in an experiment where the angle of attack was altered. Thus we could not provide the data except for $\alpha=0^\circ$. Furthermore, this mild steel aileron performed oscillations with fairly large amplitudes continuously from a Mach number as low as 0.175 up to a high Mach number, unlike other ailerons. Up to now, for example, Reference [*6*] has reported that oscillations were observed at subcritical Mach numbers, but it is not yet clear in what way such phenomena differs from what they call "transonic aileron buzz". The critical Mach number of this airfoil is about 0.725 at zero lift, and about 0.69 at $C_L=0.18$, according to Jacob's criterion. Since, additionally, the observation of actual flows ascertains the existence of the shock upon the airfoil, we may believe that at least the oscillation at the Mach number greater than 0.75 is essentially the aileron buzz. The frequency began to increase, and the amplitude began radically to decrease, near $M=0.9$. This is the Mach number at which the shock wave that has gradually moved downstream just hits the flap. In fact, it was observed from the photographs of the steady flow over the wing without the flap that the shock wave began to hit the flap position at $M=0.87$ for $\alpha=0^\circ$, 2° and 4° throughout. Consequently, the so-called "aileron buzz" is considered in this case to be the oscillations in the Mach number range from 0.7 to 0.9. The "hinoki" aileron performed irregular oscillations, and yielded data only at high Mach numbers. The reason may be as follows. This aileron model was not mechanically perfect enough and the friction effect was important. Thus, when the shock hit the flap, it was stimulated thereby and began to oscillate. Meanwhile, it is seen that the frequency makes almost no sensible change when α is changed over 0°, 2° and 4° and also when the Mach number is increased, unlike the metal flap and just like the balsa flap to be treated next. So we may adopt the frequency value of Fig. 15. The balsa aileron displayed regular oscillation, and the frequency was affected very little by the change of the angle of attack, just like the "hinoki" aileron. The lowest Mach number of buzz occurrence was the right value predicted in relation to the Mach number of shock occurrence. The Mach number at which the shock upon the upper surface reached the trailing edge was 1.0, 0.98 and 0.95, respectively, at angles at attack 0°, 2° and 4°. The frequency experienced no great change in the order of magnitude during the passage of the shock wave. Now we can see from these figures that the buzz frequency of the aileron on an identical airfoil may change greatly with the moment of inertia. Let us estimate what the value the frequency must have, if the aileron buzz behaves as claimed in Reference [*5*] or [*7*]. If we assume that the shock is located at the point of maximum thickness and that the average Mach number behind the shock is 0.7, the time for the pressure wave to go and return between the center of the aileron and the shock is calculated to be about 1/8000 seconds. And the frequency of aileron buzz should be 1000~2000 cps. But even the balsa aileron, which oscillates at the highest frequency, gives 1100 cps, and the "hinoki" and mild steel ailerons give 650 cps and 150 cps, respectively. They are about 1/7, 1/12,

1/53, respectively, of the frequencies expected from the transit times, in contradiction with the theories in References [5] and [7]. On the other hand, the moment of inertia of each aileron is calculated to be 0.0957, 0.328 and 3.97 g-mm^2, respectively, for the balsa, "hinoki" wood and mild steel ailerons, if we use the respective density values 0.132, 0.594, and 7.84 g/cm^3 for the three ailerons and take their geometrical shapes into account. The following relations are also found between the frequency and the moment of inertia.

$$1100 : 650 : 150 = \frac{1}{\sqrt{0.0957}} : \frac{1}{\sqrt{0.328}} : \frac{1}{\sqrt{3.97}}.$$

That is, the frequcency or angular velocity of such an oscillation is inversely proportional to the square root of the moment of inertia. This fact suggests that, as far as the frequency is concerned, the aileron buzz behaves just like the ordinary simple harmonic oscillations. Thus, if the aileron buzz can be described with the equation of simple oscillations, we have

$$I\frac{d^2\varphi}{dt^2} = -C\varphi,$$

where φ is the aileron deflection angle, I the moment of inertia, and C may be considered to be a constant that is determined once the airfoil and the Mach number is fixed. For example, if we take the frequency of the balsa aileron as 1100 cps, the frequencies of other ailerons are calculated as

$$n_{\text{hinoki}} = n_{\text{balsa}}\sqrt{\frac{I_{\text{balsa}}}{I_{\text{hinoki}}}} = 1100\sqrt{\frac{0.0957}{0.328}} \fallingdotseq 595 \text{ cps},$$

$$n_{\text{steel}} = 1100\sqrt{\frac{0.0957}{3.97}} \fallingdotseq 171 \text{ cps},$$

which are in fairly close agreement with the measured frequencies. The frequencies can be expressed approximately with I and C as were seen above. However, the amplitudes may have more complicated characteristics. It is clear from the fact that the larger the moment of inertia of the aileron is, the greater the amplitude becomes. In addition, the amplitude is neither divergent nor convergent and it is always a steady and stable oscillation with a fixed Mach number as is seen from Plates 5(a), (b), (c). Therefore, it may be considered to be a steady oscillation as a simple harmonic one where the damping forces due to velocity are in balance during the oscillation as was considered in Reference [9]. However, if it is so, the amplitude may be different in each case because the amplitude of a simple harmonic oscillation should depend on the initial condition which is given in the course of nature and is not always constant. As is seen from Fig. 17, however, the amplitudes of oscillations at about the same Mach number are always fixed at constant value and they do not show the voluntariness, which is true for both metal and balsa flaps. This fact suggests that the oscillation can not be considered a stable and simple harmonic one or a divergent one but a kind of nonlinear oscillation. Now, in Fig. 17, for the aileron made of "hinoki" wood, only the data at hight Mach number could be obtained, but the data with the metal flap and the

balsa flap are available over the whole range. The amplitudes of the metal flap in the region of the transonic aileron buzz are about 48 and those of the balsa flap are about 7, so the amplitudes of the metal flap are about 6.86 times as large as those of the balsa flap. On the other hand, the larger the moment of inertia is, the larger the amplitude becomes. So, considering the ratio of the moment of inertia and also the frequency,

$$\sqrt{\frac{I_{\text{metal}}}{I_{\text{balsa}}}} = \sqrt{\frac{3.97}{0.0957}} \fallingdotseq 6.44 .$$

The approximate equivalency of this ratio and the ratio of the frequency suggests the product of the freqency and amplitude to be approximately constant. In fact, their product of the metal flap is $48 \times 150 = 7200$, while that of the balsa flap is $7 \times 1100 = 7700$, so they are approximately equal.

5. Experiment 3

5.1. *Preliminary Consideration*

In experiment 2, it was discovered that the frequency of the aileron buzz was determined approximately by the moment of inertia of the aileron and a constant depending on the airfoil shape and the Mach number. We cannot define this constant explicitly unless the time lag effect of the pressure wave is made clear. At any rate, it is inferred, by the ordinary way of conjecture, that the above constant is approximately the hinge moment coefficient of the aileron. If it is so and the time lag has no severe effect, the aileron will oscillate at the frequency determined by the constant C so estimated and the moment of inertia of the aileron. Now, if we have two kinds of two-dimensional wing-aileron sets geometrically similar to each other in the airfoil but differing in the plan forms of the ailerons, and if the spans and the chords of the ailerons are A_1, A_2, B_1 and B_2, respectively, their hinge moment coefficients are connected through the following relation.

$$C_1 = \frac{A_1 B_1^2}{A_2 B_2^2} C_2 .$$

So, the frequencies are related as

$$\frac{n_1}{n_2} = \frac{\omega_1}{\omega_2} = \sqrt{\frac{C_1 I_2}{C_2 I_1}} = \sqrt{\frac{A_1 B_1^2 I_2}{A_2 B_2^2 I_1}} .$$

And, if the aileron buzz actually takes place at the frequency estimated by this formula, we shall be able to conclude that the governing constant is certainly the aerodynamically determined hinge moment coefficient and, generally, the time lag has not severe effect on the frequency.

5.2. *Model and Equipments*

The wind tunnel used in this experiment is an induction type one with a 30 cm $\times$ 30 cm cross section in the 5th Building of the Aeronautical Research Institute. A 4 m^3-high-pressure air tank is charged with air at about 150 atmospheres, which is blown out, through the settling chamber, into the part of the diffuser, where

the cross-sectional area is somewhat larger than at the test section. As the wind tunnel is of a flow-circulation type, with a covering partly open to the atmosphere, the condensation effect of the relatively dry high pressure air may be negligible. The upper and lower walls of the test section are 10 percent slotted walls as before, but the flow blown out into the plenum chamber is again absorbed into the main flow downstream contrary to the type used in experiment 2. As the optical measurement was difficult, the rod of the aileron hinge was protruded into the plenum chamber, and the rotation of the rod was picked up electrically there. The model is a two-dimensional wing with 63_3A015 section and with a plan form

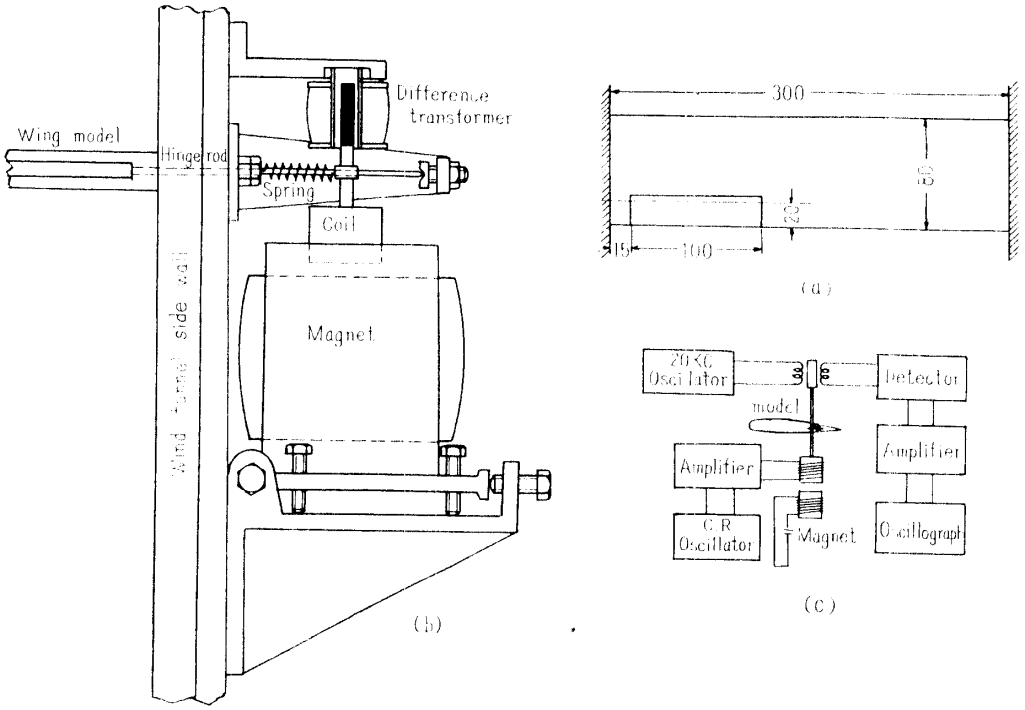

FIGURE 18. Model and circuit block diagram used in experiment 3.

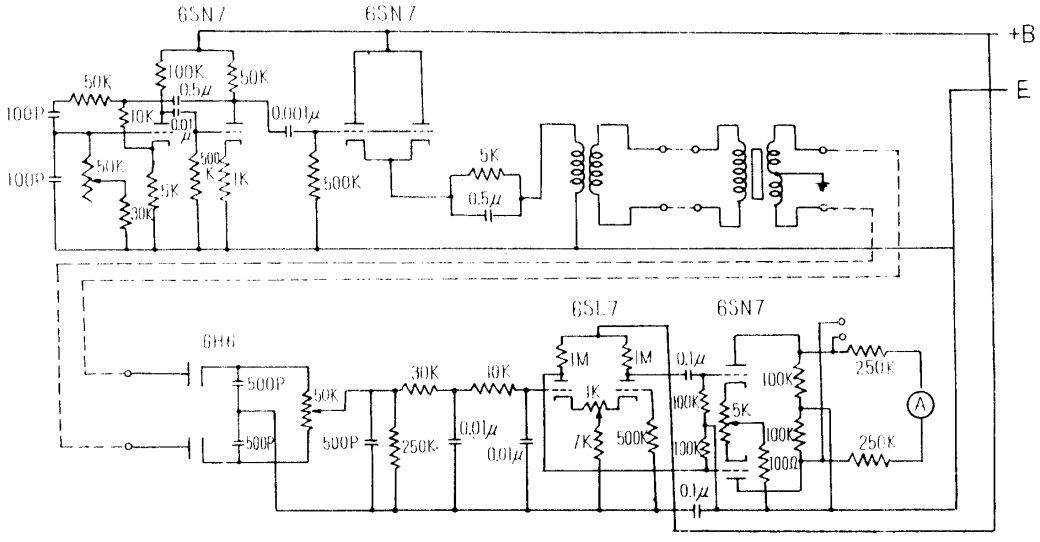

FIGURE 19. Circuit detail.

shown in Fig. 18(a), the span and the chord being 300 mm and 80 mm, respectively. For the machining convenience, the aileron, which is 100 mm span (not full-span), is attached at 15 mm from the wall. In order to accelerate the transition to turbulent flow, cemedine was pasted at the leading edge all over the span. Fig. 18(b) shows the outline of the hinge rod configuration and the circuit to detect its motion electrically. In short, the rotation of the rod is converted into the displacement of the ferrite core, and the latter is picked up by the difference transformer. The spring in the figure was omitted in this experiment, as well as the

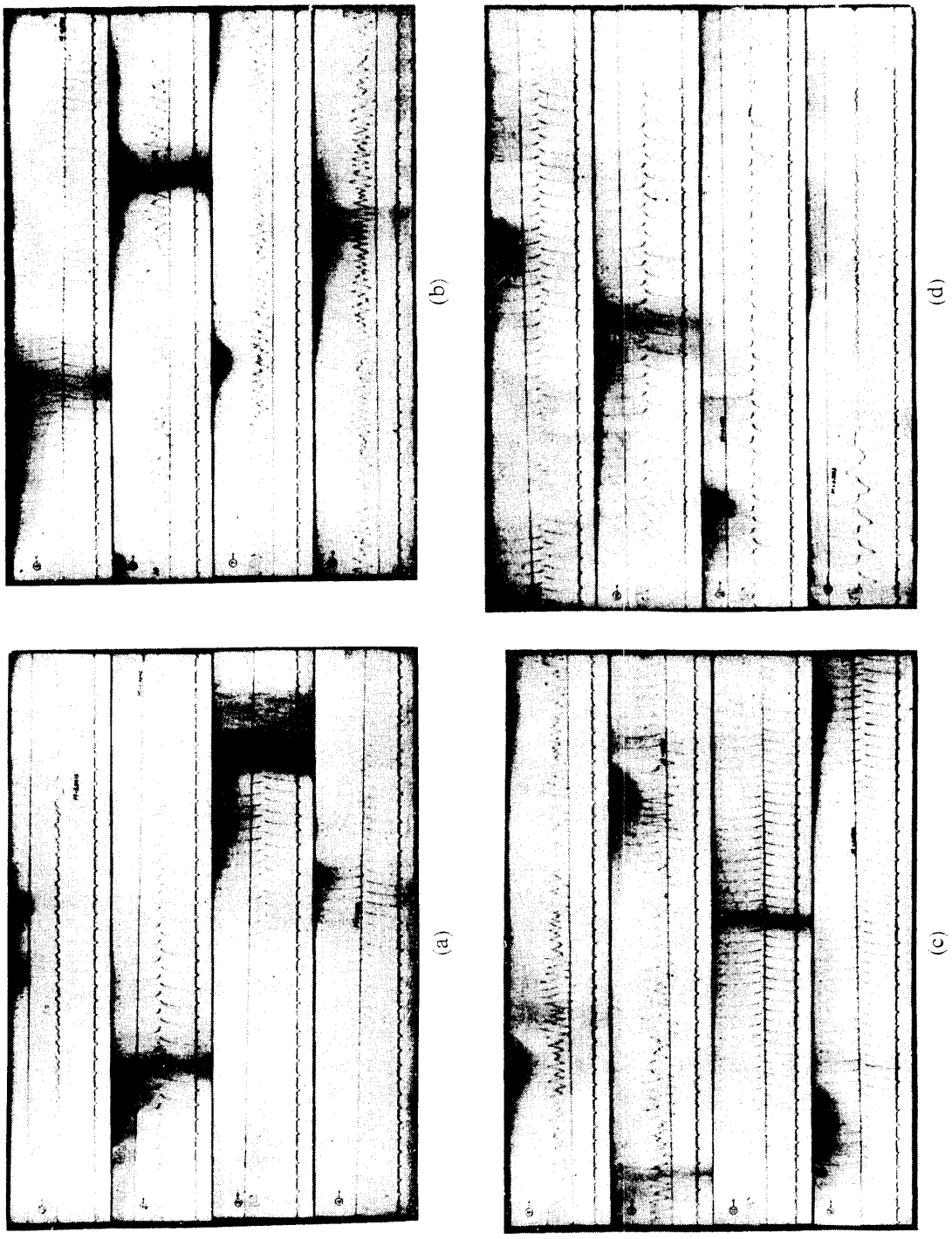

PLATE 6.

mass balance of the aileron. The magnet and the exciter coil is for the setting in no-wind condition and the calibration, but is not necessary in the actual measurement. Fig. 18(c) is the block diagram of the circuit. Fig. 19 gives its detail. The 20 kc carrier wave is fed to the difference transformer, is modulated in amplitude by the ferrite core displacement, and the resultant waveform is recorded, after detection and amplification, on the electromagnetic oscillograph.

5.3. *Results and Discussion*

Two kinds of ailerons were made, the one of 56S alloy with density 2.865 g/cm^3 and the other of balsa. For the balsa aileron, however, the amplitude of oscillation was too small to be detected by the measuring equipment because of its small moment of inertia. Plate 6 shows a typical long-time record by the oscillograph of the 56S aileron equipped with the calibrator coil. Here, again, the oscillations at low speed is also discernible, as remarked in experiment 2, but those at high Mach numbers may be essentially the buzz phenomena. Figs. 20 and 21 show the curves relating the aileron buzz frequency with the Mach number measured on the 56S aileron at angles of attack 0°, 2° and 4°, without and with the coil,

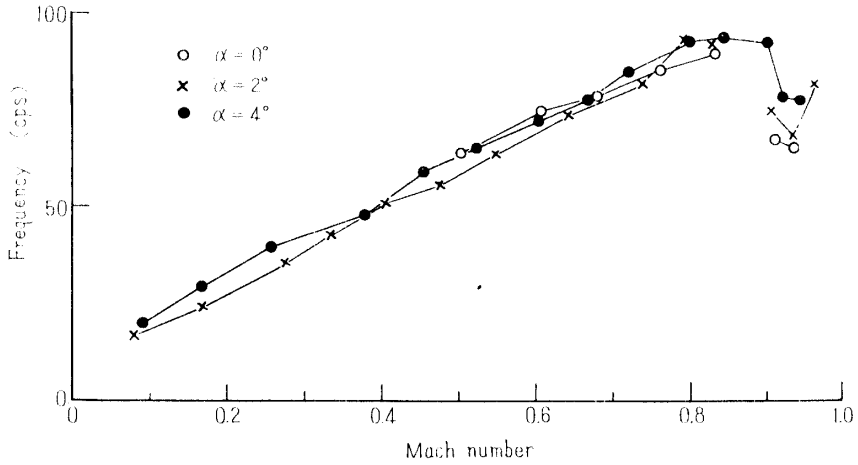

FIGURE 20. Buzz frequency versus Mach number (without coil).

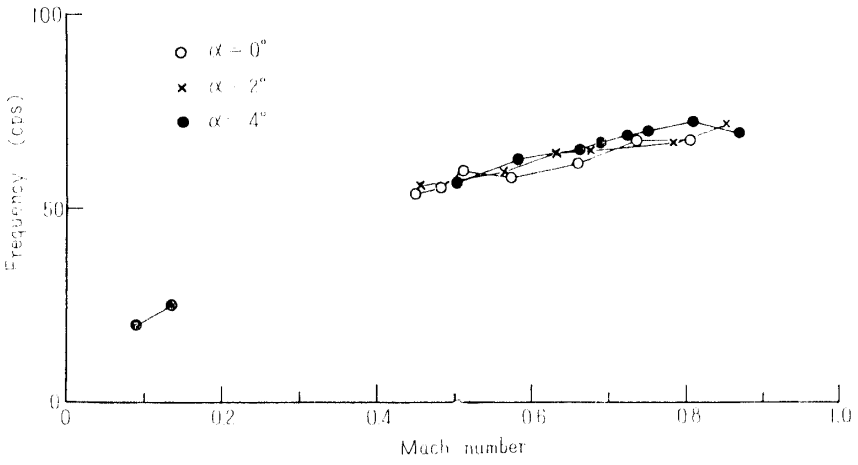

FIGURE 21. Buzz frequency versus Mach number (with coil).

respectively. It is found, from these figures, that the frequencies without and with the coil are about 80 to 90 cps and 70 cps, respectively. Meanwhile, the moment of inertia of this aileron is calculated approximately to be 1126 g-mm^2. So, the frequency is predicted, on the basis of the results of experiment 2, as follows. For the aileron of experiment 2, $A_2=36$ mm and $B_2=5$ mm, while for the present one $A_1=100$ mm and $B_1=200$ mm. Using $n_{2\,\mathrm{steel}}=150$ cps, $n_1=60$ cps. Using $n_{2\,\mathrm{hinoki}}=650$ cps, $n_1=74$ cps. And, using $n_{2\,\mathrm{balsa}}=1100$ cps, $n_1=68$ cps. On the average, n_1 must be about 70 cps for the aileron without coil. The frequency obtained, 80 to 90 cps, deviates 15$\sim$20 percent from this value, but it can be considered as a reasonable result. The deviation may be attributed to the error in the moment of inertia estimation, the precision error of the model, the aerodynamic dissimilitude coming from the use of different plan forms of the model as well as the the change in Reynolds number, the difference of the time lag, and the difference in characteristics of the wind tunnels used. Thus it may be safe to conclude that the constant C is the aerodynamic hinge moment determined almost entirely by the airfoil shape and the Mach number. The greatest cause imaginable of the above-mentioned error except the one from the time lag is the difference in the wind tunnels used, especially that in the area ratio of the test section and the model. The greater the area ratio, the higher pressure the wing may be subjected to. We can make a correction, for example, after Reference [*11*] as follows. If a doublet of a certain intensity is located at the wing position, the pressure increment at an arbitrary point, for example at the point on the wall just above the trailing edge, may be calculated. We can make a rough estimation of the area-ratio effect by considering that the pressure upon the aileron, and so the hinge moment coefficient is altered just by this pressure increment ratio of the specified wind tunnel. Following this line, and denoting the constant C in experiments 2 and 3 with C_2 and C_3, respectively, we have

$$C_3=\frac{1.4}{1.55}\left(\frac{376}{300}\right)^2 C_2=1.42C_2\,.$$

Thus we obtain

$$n_3=\sqrt{1.42}\times 70=83\ \mathrm{cps}\,.$$

This values is comparable with the measured frequency. While, if the time lag can be expressed as $t=\delta^2/25\nu$, the delay time of this model is about 4 times as large as that of the model in experiment 2, because the scale of this model is 4 times the one in experiment 2 and then the boundary layer thickness δ is duplicated. Besides, the frequency of this model being less than about 1/2 times, the period is more than about 2 times and therefore the phase difference must be less than about 2 times compared with that of the previous experiment. Nevertheless, the frequencies could be determined reasonably from the previous experiment data. Therefore, it can be considered that the constant C may be an aerodynamic hinge moment coefficient as can be determined approximately by the airfoil and Mach number.

Furthermore, for the aileron with the coil the moment of inertia is increased

to about 1863 g-mm^2. Therefore, assuming the frequency without the coil to be 90 cps, we have the predicted value $n=70$ cps, which agrees well with the experimental result. Thus, if we use the same wind tunnel and the same model throughout, the frequency will certainly be inversely proportional to $\sqrt{I}$, and the constant C, which appears therein, will be a factor depending exclusively on the airfoil shape and the Mach number and almost independent of the time lag, provided the aerodynamic conditions are the same.

6. Experiment 4

6.1. *Preliminary Consideration* .

It has been found from the foregoing experiments that the aileron buzz frequency is almost entirely determined by the hinge moment coefficient and the moment of inertia of the aileron. The experiment described in this chapter was planned with the following aims by the use of the induction type wind tunnel and the interferometer apparatus at Tamaki Laboratory of the Institute of Industrial Sciences: to measure the absolute value of the hinge moment for each deflection angle both in the buzz state and in the steady flow state, to get numerically from these results the time difference for steady and unsteady flows, and thus to recheck the foregoing results obtained with airfoils with different sizes as well as to acquire further more detailed data.

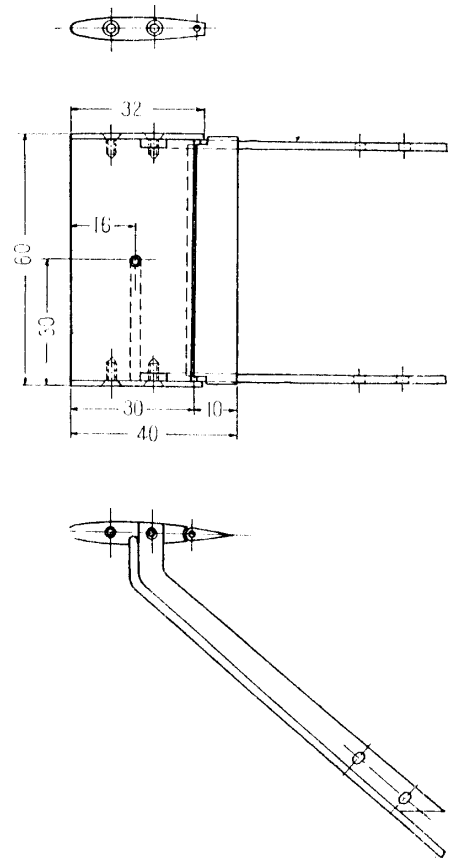

Figure 22. Model used in experiment 4.

6.2. *Model and Equipments*

The wind tunnel used is of an induction type with a 100 mm × 60 mm cross section. It is not of a circulation type, and the air charged at below 10 atmospheres in a 10 m^3 high-pressure tank is injected into the diffuser under the regulation with valves. The upper and lower walls of the test section are not slotted as in the previous experiments, but solid. The Mach number is controlled by regulating the injected air pressure with valves, and is measured at a standard position apart from the model with a pressure hole. A 63_2A015 airfoil was used as before, and the support and the aileron were attached as illustrated in Fig. 22. The span and the chord of the airfoil were 60 mm and 40 mm, respectively, and two kinds of ailerons over full span, made of 56S and balsa respectively, were prepared. The measurement consisted of photographing the interferometer fringes with a drum-type high-speed rotating camera and photographing the interferometer pattern of the steady flow at fixed aileron deflection angles.

6.3. *Results and Discussion*

The maximum Mach number available in this experiment was about 0.8. Up to this Mach number the balsa aileron and even the metal aileron revealed little indication of oscillations. A feeble oscillation could be recorded only once at the angle of attack about 4°. Then the shift of the interferometer fringe was not at all perceptible, and the expected data could not be obtained. The Mach number in this case was 0.747, and the measured frequency was 223 cps. Using this value and the calculated moment of inertia of the aileron, which was 43.7 g-mm^2, we have

$$C = 4\pi^2 n^2 I = 8.605 \times 10^7 \text{ g-mm}^2/\text{s}^2 .$$

Consequently, we can estimate the moments, for example, for the aileron deflections 3°, 6°, 9° as

$$M_{3^\circ} = 4.5 \times 10^4 \text{ g-cm}^2/\text{s}^2 ,$$
$$M_{6^\circ} = 9 \times 10^4 \text{ g-cm}^2/\text{s}^2 ,$$
$$M_{9^\circ} = 13.5 \times 10^4 \text{ g-cm}^2/\text{s}^2 .$$

In order to check this result, photographs were taken of the steady flow with aileron deflection angle fixed at the above-mentioned values. One example ($\varphi = 6^\circ$) is illustrated in Plate 7. The hinge moment calculated from this is plotted in Fig. 23. As is seen from the figure, the order of magnitude of the constant C agrees approximately with the hinge moment coefficient in the steady state flow, but the absolute values are considerably different from each other and the ratios of the hinge moment during oscillation to that in steady flow at the deflection angle 3°, 6°, 9° are 0.65, 0.71 and 0.48, respectively. However, the frequencies are not so much affected because of the proportionality to the square root of the hinge moment and, for example, the frequencies based on the hinge moment in steady flow are 274, 266 and 322 cps, respectively, which are comparable with the measured frequency. The difference of the frequencies during oscillation and in steady flow is, of course, due partly to experimental errors such as the installation

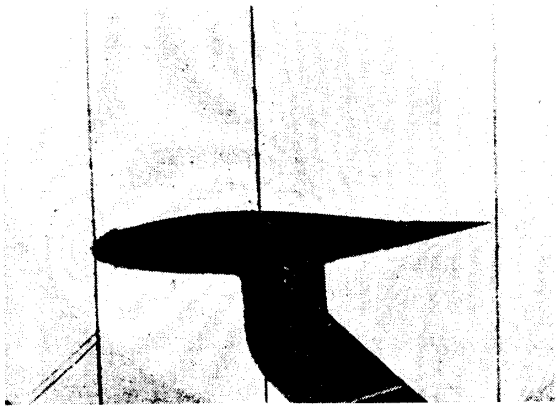

PLATE 7.

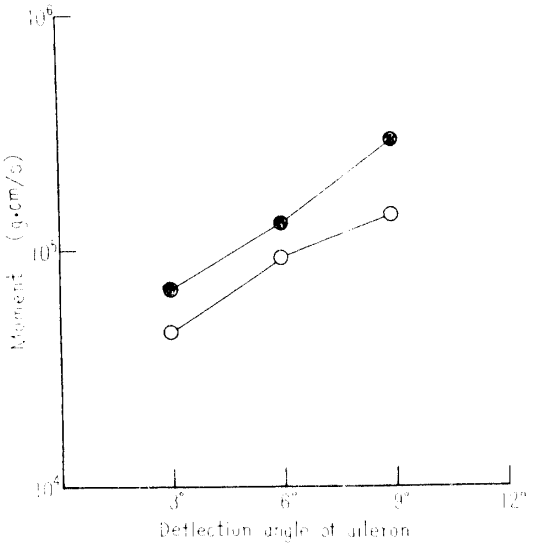

FIGURE 23. Hinge moment in steady flow and in buzz.

angle of the aileron, but the main cause is probably the phase lag of the hinge moment vector and the deflection angle vector which is not exactly 180°. It is conjectured from this fact and the reason described in Chapter 4 that the aileron buzz is certainly a nonlinear oscillation in the unstable region. However, it can be concluded that the approximate values of the frequencies do not differ considerably from the value calculated on the basis of the hinge moment coefficient in steady flow.

The buzz frequency of this aileron may also be estimated by the application of the same method as in Chapter 5. Choosing the frequency of the steel aileron in experiment 2 as a standard, we have

$$n \fallingdotseq 150\sqrt{\frac{60\times 40^2\times 3.97}{36\times 5^2\times 43.7}} \fallingdotseq 117\ \text{cps},$$

while, making use of the result of experiment 3, we have

$$n \fallingdotseq 90\sqrt{\frac{60\times 10^2\times 1126}{100\times 20^2\times 43.7}} \fallingdotseq 177\ \text{cps}.$$

Either of these is below the measured value. This may be due to the wind tunnel effect as we have discussed in experiment 3. Since the wind tunnel walls are solid and the area ratio of the model is very large, such a result may be natural. The estimation making use of the results of Reference [*11*] yields the following numerical relation between the hinge moment coefficients for solid wall and slotted wall wind tunnels in experiment 2

$$C_{2\,\text{solid wall}} = \frac{4.1}{1.55} = C_{2\,\text{slotted wall}} = 2.65\,C_{2\,\text{slotted wall}}.$$

Then, if the conversion is made from the solid wall of this scale to that of the present scale, we can obtain the coefficient C_4 as

$$C_4 = \frac{2.8}{4.1}\left(\frac{188}{100}\right)^2 C_{2\,\text{solid wall}} = 6.38\, C_{2\,\text{soltted wall}}\,.$$

So, we have

$$n_4 = 117 \times \sqrt{6.38} = 293\ \text{cps}\,.$$

This is considerably larger than the measured value, being no more than a rough estimation. At any rate, we see how vitally the wind tunnel-model interaction affects the buzz frequency.

7. Experiment 5

7.1. *Preliminary Consideration*

The vibration system considered up to the present has been restricted to a wing-aileron system for simplicity, but in certain cases, for example in Reference [5], the springs may be attached to the wing-aileron system. According to the results obtained in Reference [5], the spring constant had not any effect on the state of the aileron buzz. But it is apparent that this statement is not always correct, because the aileron can be fixed in fact with a very stiff spring. Therefore, in this experiment, the effect of spring stiffness on the aileron oscillation is studied with various stiffness to a larger extent than that used in Reference [5]. In addition, as was made clear in Experiment 1, the delay time of the pressure wave caused by the aileron deflection required to come back again is affected largely by the separated boundary layer. Therefore, it is supposed that the delay time may be changed with a model devised so as to thin the boundary layer thickness on the surfaces, hence the change of the oscillation pattern or, in the extreme case, the possibility to prevent the oscillation may be expected. Inversely, if it is practically possible, the large effect of the thick boundary layer on the delay time will be concluded. In this Chapter, a wing with slotted surfaces was used in order to thin the boundary layer.

7.2. *Model and Equipments*

The wind tunnel used for these two kinds of experiments is the same as that used in experiment 3, and is an induction-type wind tunnel with a 30 cm × 30 cm test section. The wing with the spring is the one with solid surface used previously, and the mechanical shape of the spring is as is shown in Fig. 24(a). The springs used are three kinds of cylindrical helical springs and the mechanical conditions are as follows:

Spring No.	Diameter of wire (mm)	Radius of spring (mm)	Number of turns	Pitch (mm)
1	0.5	3	8	2.5
2	1	3.5	7	2.67
3	1.4	3.75	7	2.37

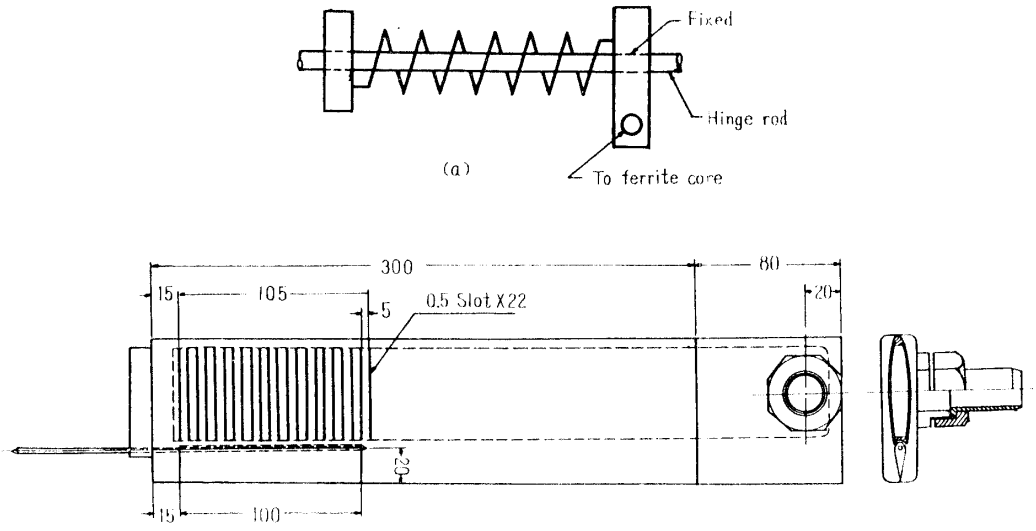

FIGURE 24. Model used in experiment 5.

The aileron is made of an alloy 56S, and the experiments were performed with the coil which was used for the calibration. The slotted wing has NACA 63_2A015 airfoil profile and the plan forms of the wing and the aileron are the same as that of the solid wing. But, as is seen from Fig. 24(b), it has many slots on the part of the wing before the aileron. The width of the slot is 0.5 mm and its opening ratio is 10 percent. The air removed through these slots are sucked outside through the hollow wing with a 20 HP vacuum pump which is of a blower type. But this vacuum pump was not sufficient for the purpose. The aileron is the same as before and the coil used for the calibration is kept attached.

7.3. *Results and Discussion*

The white circles in Figs. 25 to 27 inclusive represent the frequency-to-Mach number curves obtained with the wing-aileron-spring 1 system at angles of attack $\alpha=0°$, 2° and 4°, respectively. As is seen from these figures, the manner of the

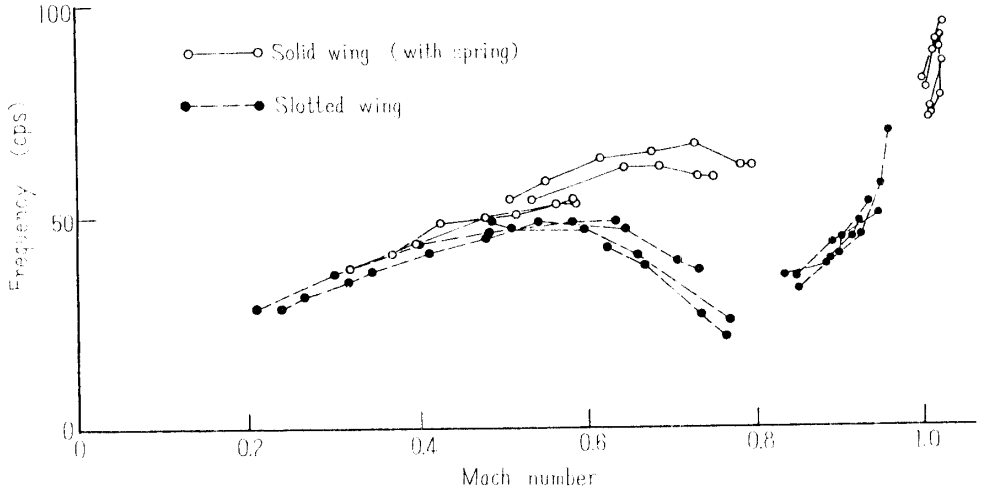

FIGURE 25. Buzz frequency versus Mach number ($\alpha=0°$).

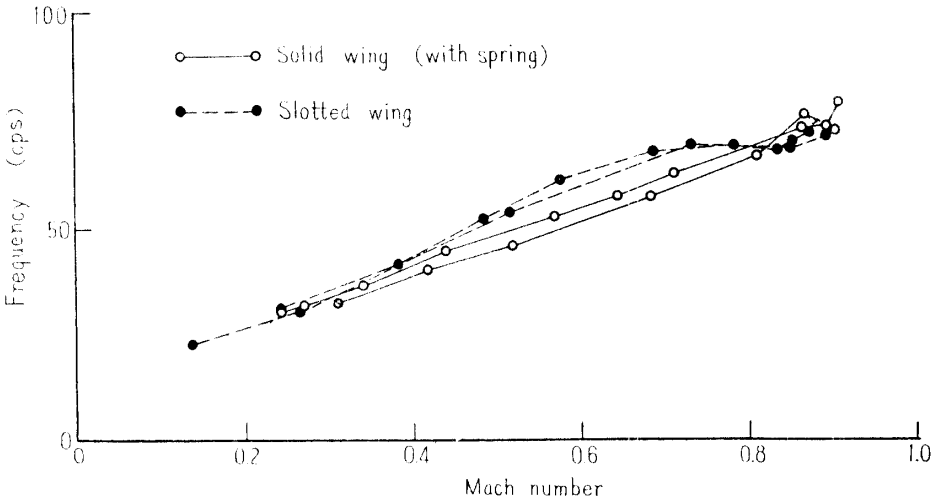

FIGURE 26. Buzz frequency versus Mach number ($\alpha = 2°$).

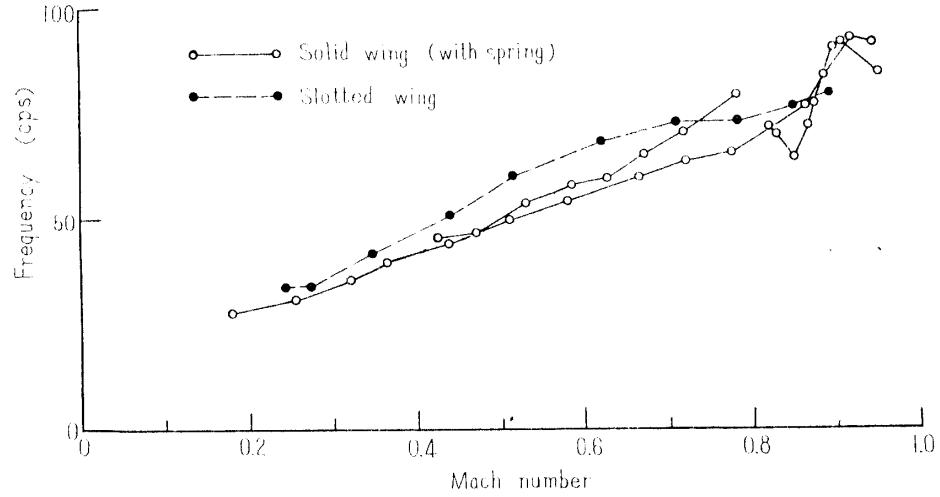

FIGURE 27. Buzz frequency versus Mach number ($\alpha = 4°$).

oscillation is almost independent of the angles of attack and the frequencies are almost the same as those of the wing-aileron system without spring (Fig. 21), thus they show that the spring does not affect the oscillation. However, the systems with spring 2 or 3 showed no oscillations measurable with this equipment throughout the transonic speed range. Now, comparing the spring constants with the magnitude of the hinge moment coefficient of this wing-aileron system, the hinge moment coefficient is

$$C = 4\pi^2 n^2 I = 4\pi^2 \times 90^2 \times 1126 \fallingdotseq 3.6 \times 10^8 \frac{\text{g-mm}^2}{\text{s}^2}$$

with the use of the result from experiment 3. On the other hand, the spring constant calculated is

$$k = \frac{d^4 \cos\alpha}{64nR\left(\dfrac{\sin^2\alpha}{G} + \dfrac{2\cos^2\alpha}{E}\right)},$$

where d is the diameter of the wire used, R the radius of the spring, n the number

of turns, α the helical angle, E the Young's Modulus, and G the modulus of rigidity. From this equality the sprihg constant, k_1, k_2 and k_3 are given as

$$k_1 = 0.0413 \times 10^8 \text{ g-mm}^2/\text{s}^2,$$
$$k_2 = 0.656 \times 10^8 \text{ g-mm}^2/\text{s}^2,$$
$$k_3 = 2.272 \times 10^8 \text{ g-mm}^2/\text{s}^2.$$

Hence

$$k_1/C = 1/87,$$
$$k_2/C = 1/5.5,$$
$$k_3/C = 1/1.6.$$

The sum of the hinge moment vector on the wing-aileron system is in unstable region owing to the time lag and the moment vector due to a spring, which is 180° out of phase with the aileron position is also in unstable region, but the greater the spring moment is, the nearer the sum vector to the boundary of the stable and unstable region is. The wing used in this experiment is the same with that used in experiment 3, except the attachment of a spring, so the aerodynamic characteristics are unchanged and the hinge moment coefficient C in steady flow is also invariable. As was made clear in Chapters 5 and 6, the deviation from the hinge moment vector of a stable, simple harmonic oscillation is also small, so the effective hinge moment coefficient of the system with spring must be approximately $C+k$, and the frequency will become large. Moreover, as will be discussed in next chapter, the product of the frequency and amplitude is constant also in this case and equal to that of the no-spring system, hence the amplitude of a wing-aileron-spring system becomes small. Therefore, a regular oscillation measurable could not be detected with the stiff spring, probably because the amplitude of the system was decreased with the use of a spring and the system was apt to suffer

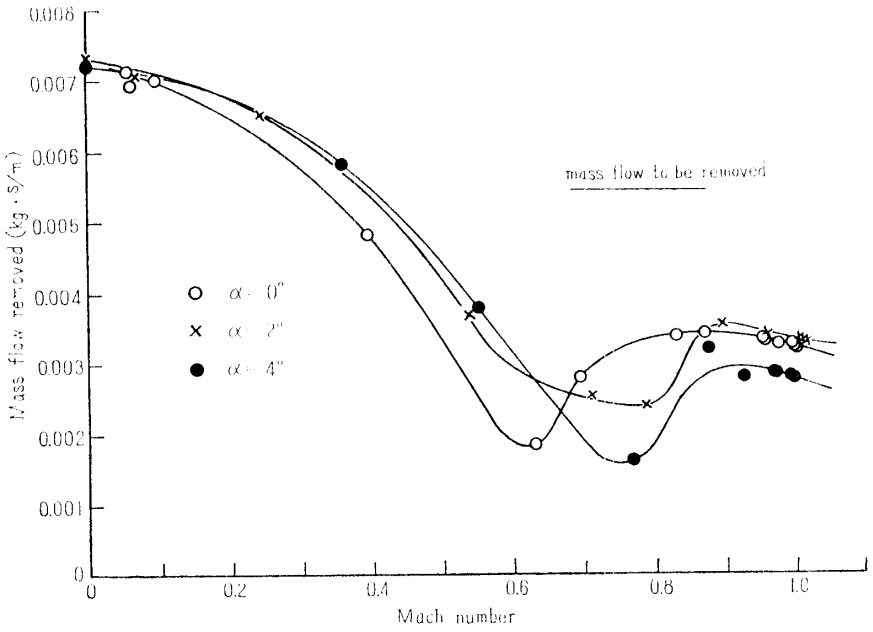

FIGURE 28. Mass flow removed.

an effect of disturbances near the boundaries of the stable and unstable regions. Further, the motion of the ferrite core was required not only in the vertical direction but also more or less in the horizontal direction, so the irregularity of motion

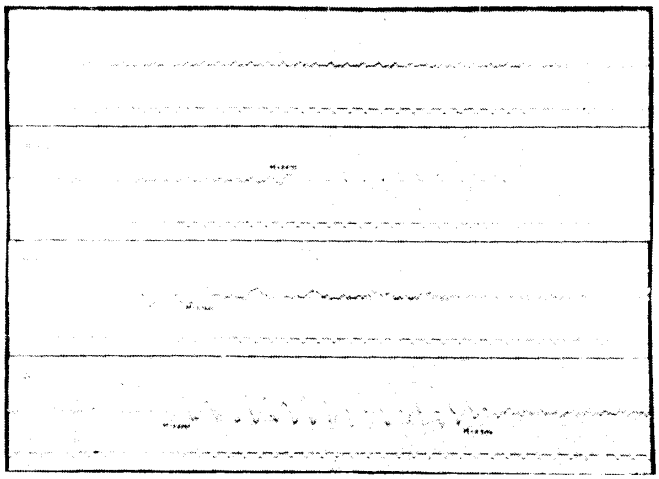

(a)

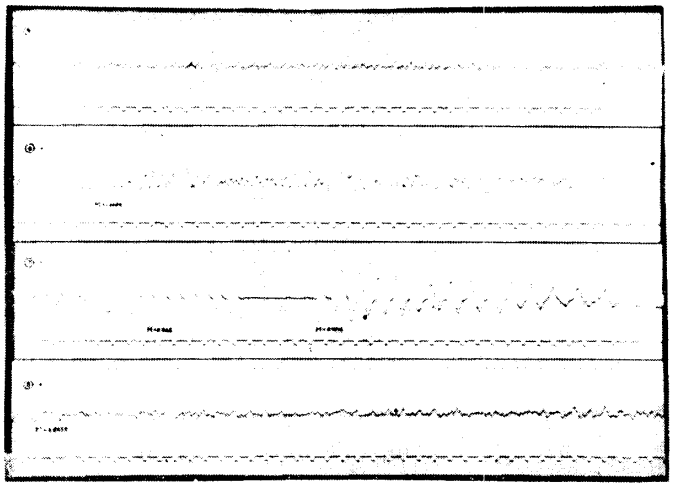

(b)

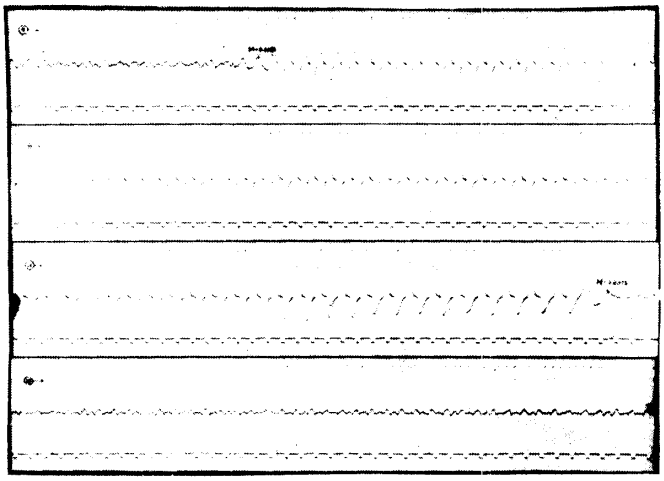

(c)

PLATE 8.

of the core increased when the movement decreased slightly and this perhaps largely affected the measured oscillation pattern.

Next, the black circles in Figs. 25 to 27 inclusive represent the frequency-to-Mach number curves obtained with the slotted wing at angles of attack $\alpha=0^\circ$, 2° and 4°, respectively. Fig. 28 shows the curves showing the mass flow removed through the slots on the surfaces in terms of Mach number, and the solid line parallel to the horizontal axis represents the mass flow to be removed, which is derived from the same idea as in experiment 1. The power of the pump is not sufficient to suck the required mass flow in the transonic speed range. The mass flow removed is only $1/2\sim1/3$ times as that desired. However, the curve at angle of attack 0° represents clearly the change in the frequency. In the cases of $\alpha=2^\circ$ and 4°, the suction has almost no effect. The reason for this is probably that, the larger the angle of attack α is, the stronger the separation on the upper surface of the wing becomes, so that the pressure on the upper surface decreases, reducing the suction effect on the state of the surface. Plate 8 shows a part of this record, and from this record, it is apparent that not only the frequency but also the amplitude changes and particularly the oscillation has disappeared in the Mach number range where the so-called aileron buzz is severe. Drawing in the boundary layer flow through the slots on the surfaces of a wing, the flow pattern and the various aerodynamic characteristics must change, and it corresponds to a deformation of the airfoil, hence it may be considered that the change of the effective airfoil shape is the main cause of the disappearance of the aileron buzz. On the other hand, it may be considered also that the main cause is the decrease of the delay time owing to the suction of the thick boundary layer flow and then the moment vector comes back to the stable region. Considering the facts that the states of vibration with the slotted wing at angles of attack $\alpha=2^\circ$ and 4° were almost the same as obtained with the solid wing, that all the wings tested in many references experienced the aileron buzz, and that the aileron buzz occured practically with the solid wing at angle of attack $\alpha=0^\circ$, which is not so different from the slotted wing in the aerodynamical characteristics, it is most appropriate to consider that the main cause of the disappearance of the aileron buzz with the slotted wing is the decrease in delay time large enough to take up the hinge moment vector from the unstable region owing to the decrease in the thickness of the boundary layer flow.

8. Overall Discussion

Some characteristics of the aileron buzz have been clarified by the experiments described above. Generally, the transonic aileron buzz is a very stable, sinusoidal oscillation, of which frequency and amplitude are fixed constant at a given wing and a given Mach number. However, if it is a stable, simple harmonic oscillation as was assumed in Reference [9], the amplitude may be different in each case and it is unnatural to consider various disturbances so as to give the same initial condition constantly, hence these aileron oscillations should be in the unstable

region. If the operating hinge moment is a linear type, the oscillation should always diverge, while the experimental result is not so, thus it is concluded that the aileron oscillation should be that of the non-linear type. In addition, according to the results obtained from experiment 2, there exists a relation $An=$ constant between the frequency n and the amplitude A of the aileron attached to the same wing, if the frequency n is varied by the change in the mass moment of inertia of the aileron. Therefore, it is conjectured that the differential equation governing the phenomena of the aileron buzz is a nonlinear one so as to give the relation $An=$constant. Such a nonlinear equation can not be discussed generally as far as the general characters of the nonlinear equations can not be clarified, but it is known among the important nonlinear differential equations studied up to the present that the one including the terms of φ, $\dot{\varphi}$ and $\dot{\varphi}^3$ corresponds to the one required. Namely, it can be proved that the oscillation system of the form

$$\ddot{\varphi} = -C\varphi + D\dot{\varphi} - E\dot{\varphi}^3$$

takes a periodic motion after the initial transient has ceased, provided the terms $D\dot{\varphi}-E\dot{\varphi}^3$ are comparatively small and C, D and E are positive constants, then the frequency and the amplitude can be written as follows:

$$n = \frac{\sqrt{C}}{2\pi},$$

$$An = \frac{1}{\pi}\sqrt{\frac{D}{3E}}.$$

The inevitability of the equation governing the aileron buzz to take this form can not be proved, but we will analyse the detailed record during oscillation obtained in Reference [9] in order to illustrate that the equation probably has such a form. The configuration of the aileron motion with time is given in Reference [9], so $\dot{\varphi}$ corresponding to each φ can be calculated numerically. The total aerodynamical hinge monent acting at angle φ during oscillation is also given in Ref. [9], so the excess hinge moment can be obtained by subtracting the one in the steady flow from the above one. The calculated resluts in each case, in which a direction of the aileron motion is taken positive or negative because of the ambiguity of the positive direction of the aileron angle in Ref. [9], are shown in Fig. 29. The excess hinge moment still has a phase lag for $\dot{\varphi}$ and depends upon the higher differential coefficients. However, in order to simplify the discussion, substituting an open curve through the origin and two black circles in the figure for the closed curves, the equation including only the terms of $\dot{\varphi}$ and $\dot{\varphi}^3$ is as follows:

$$HM = 18.016\times10^{-2}\dot{\varphi} - 29.095\times10^{-8}\dot{\varphi}^3,$$

where the units of the hinge moments, the aileron deflection and the time are in lb, degree and second, respectively, and the coefficients have the proper dimensions. Morever, the hinge moment due to the damper used in this experiment is 168/704 times as large as the aerodynamic one, so the equation of this oscillation is as follows:

$$I\ddot{\varphi} = -13.563\varphi + 13.717\times10^{-2}\dot{\varphi} - 29.095\times10^{-8}\dot{\varphi}^3.$$

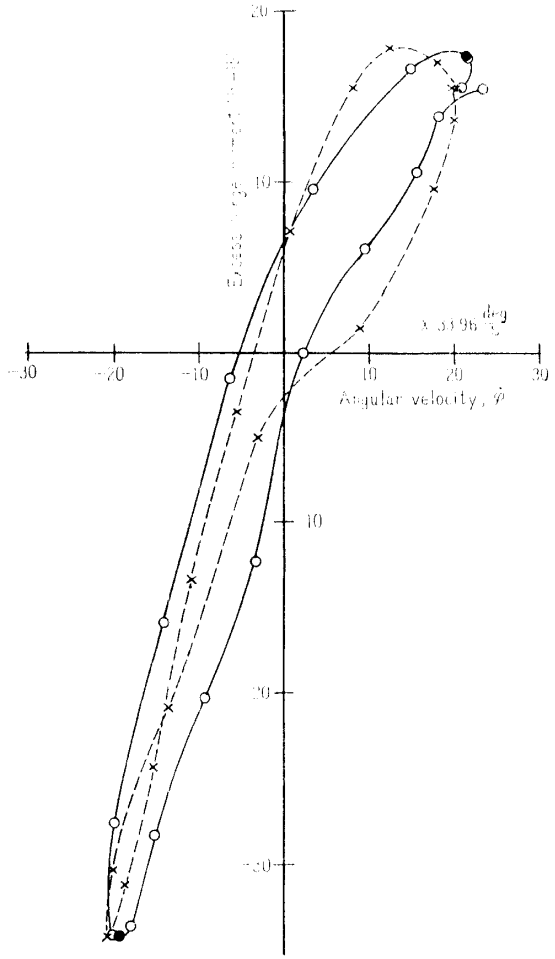

FIGURE 29. Excess hinge moment versus angular velocity.

Hence,

$$An = \frac{1}{\pi}\sqrt{\frac{13.717\times10^{-2}}{3\times29.095\times10^{-8}}} = 126.1\,\frac{\text{deg}}{\text{s}}\,.$$

On the other hand, as the frequency and amplitude of this oscillation are about 20.5 cps and 5.5 degress respectively, then

$$An = 20.5\times5.5 = 112.75\,\text{deg/s}\,.$$

Both of the products An agree well with each other. Therefore, it is believed to be correct to conjecture that the aileron buzz phenomena may be described by a nonlinear differential equation including the term proportional to $\dot{\varphi}^3$. However, considering these experimental data only, it is not obvious in what mechanism such a moment occurs. Perhaps, the variation of the extent of the separated boundary layer following the shock wave movement affects the aeroynamic damping moment as a third-order effect. Therefore, under a state of oscillation in the unstable region, the term concerning $\dot{\varphi}^3$ largely affects the oscillation pattern. However, it is supposed that the term of $\dot{\varphi}^3$ has little effect on the origination of the aileron buzz and that the mechanism of the occurrence of the aileron buzz may depend mainly upon the terms of φ and $\dot{\varphi}$. Namely, a stable system governed by the equation

$$I\ddot{\varphi}(t) = -C\varphi(t) - D\dot{\varphi}(t)$$

may become unstable owing to a delay time.

Taking only the essential delay time into account, the above oscillation system becomes as follows in the transonic speed range :

$$I\ddot{\varphi}(t) = -C\varphi(t-\tau) - D\dot{\varphi}(t) .$$

Further, according to the experimental results, the delay time τ is small compared with the period, so the approximate form of the above equation is

$$I\ddot{\varphi}(t) = -C\varphi(t) + (C\tau - D)\dot{\varphi}(t) .$$

As is seen from this equation, the coefficient of $\dot{\varphi}$ is negative enough to stay the system in the stable region, provided the delay time is small, but if the shock wave appears on the surfaces in the transonic speed, the delay time as well as the thickness of the boundary layer becomes large. As the Mach number increases, the strength of the shock wave and the thickness of the boundary layer increase and the corresponding delay time also increases. Finally, as the coefficient of $\dot{\varphi}$ becomes positive, the system becomes unstable and begins to oscillate. It is due to this reason propably that the actual buzz occurs at the Mach number slightly higher than the critical Mach number, $M_{\text{crit.}}$. After the oscillation began, the frequency and amplitude of a wing-aileron system at a given Mach number depend not only upon the aerodynamic coefficients, but also upon the delay time τ, and τ is concerned with the character of the wing surface and the Reynolds number, so the measurement of τ as well as the aerodynamic coefficient is required to predict the configuration of the oscillation. To check the above statement based on the measured value of I, C, D, E, τ for an actual wing-aileron system has not been performed in this paper and the studies of their detailed characteristics have been left open to the future work. Practically, however, it is desirable to prevent the aileron buzz. The large-amplitude oscillations are very dangerous. As a fundamental method to prevent the aileron buzz, it is the best way to reject the entering the system to the unstable region. To do so, it can be considered useful to devise the changes of C and D by the proper deformation of the airfoil, but it may be somewhat difficult because almost all the wings tested up to the present experienced the so-called aileron buzz. Hence, it is believed that the best way is to suck out the thick boundary layer on the wing surfaces, and thus to make the corresponding delay time small enough to eliminate the aileron oscillation. In the case of the conventional solid wing, the amplitude can be highly decreased also either by decreasing the mass moment of inertia of the aileron as was proved experimentally in experiment 2 or by attaching a stiff spring as was seen in experiment 5.

9. Conclusion

In experiment 1 it was pointed out that, when a disturbance is applied, it takes a finite time, which may depend upon the boundary layer thickness, for the flow in the region of shock-boundary layer interaction to reach the new state to be brought about by the disturbance, that the delay time, which is the sum of this and the go-and-return time of the disturbance with the sonic velocity, constitutes the main cause of the buzz, and that the theories developed in other re-

ferences, which are based on the go-and-return time with the sonic velocity only, are inadequate because this is generally smaller than the boundary layer resettling time.

The last argument was also demonstrated by the observation of the actual buzz in experiment 2. It was made clear, furthermore, that the frequency of the aileron buzz is independent of the go-and-return time and is inversely proportional to the square root of the mass moment of inertia of the aileron and that the amplitude is uniquely determined by the kind of aileron and the Mach number, admitting no arbitrariness to be introduced by the initial conditions. Thus it was indicated that the buzz may be an oscillation subject to some nonlinear hinge moment. In experiment 2 it was also discovered that, for the identical airfoil and the equal Mach number, the product of the frequency, which varies with the kind of aileron i.e. with the mass moment of inertia, and the corresponding amplitude is nearly constant. In experiments 3 and 4 it was made clear that the constant for predicting the frequency is approximated by the hinge moment coefficient to the aileron in steady flow, and consequently that, even for an oscillation in the unstable region, the magnitude of the terms concerning $\dot{\varphi}$ is not so large compared with the hinge moment in steady flow. In Experiment 5, in the first place, the effect of the spring was investigated, and it was shown that the spring is not wholly ineffective, differing from the claim of the other reference, and that, naturally, the frequency increases and the amplitude decreases as the spring stiffness increases. The annihilation of the aileron buzz is experimentally realized by the suction of the thick boundary layer on the surfaces through the slots on the airfoil. So it was concluded that the time lag causing the aileron buzz is largely dependent on the time lag due to the presence of the thick boundary layer. From the experimental evidences described above, it was indicated that the equation governing the state of the aileron buzz is a nonlinear differential equation containing the hinge moment, which is proportional to the third power of the angular velocity of the aileron. The validity of this statement was given by the analysis of the data of Reference [9]. It was also pointed out that, for the understanding of the aileron buzz occurring on an actual airfoil, the acccurate data of the time lag as well as of the aerodynamic coefficient are required. But we must expect the details of these values only from the future studies. It was also concluded that the following are effective as general methods of preventing the aileron buzz: 1. To suck out the thick boundary layer induced by the shock wave by some means, making it sufficiently thin, and thus to reduce the corresponding delay time. 2. To increase the frequency and thus to decrease the amplitude either by decreasing the mass moment of inertia of the aileron or by attaching a stiff spring.

Acknowledgement

The study has been carried on and completed under the guidance of Professors S. Kawada and R. Kawamura at Aeronautical Research Institute, University of Tokyo, to whom the author's highest acknowledgement is made for their helpful

advices and encouragement throughout the study. The author is also greatly indebted to Professors I. Tani, F. Tamaki, J. Kondo, K. Washizu, and Messrs. M. Komoda and S. Yui.

References

[1] Marvin Pitkin, William N. Gardner and Howard J. Curfman, Jr.: Observations on an Aileron Flutter Instability Encountered on a 45° Swept-Back Wing in Transonic and Supersonic Flight. NACA RM L6L09.

[2] A. L. Erickson and R. L. Mannes: Wind Tunnel Investigation of Transonic Aileron Flutter. NACA RM A9B28.

[3] Harold L. Crane: An Investigation of Aileron Oscillations at Transonic Speeds on NACA 23012 and NAKA 65-212 Airloils by the Wing Flow Method. NACA RM L8K29.

[4] Lionel L. Levy, Jr., and Earl D. Knetchel: Experimental Study of the Effect of Sweepback on Transonic Aileron Flutter. NACA RM A51E04.

[5] Sherman A. Clevenson: Some Wind Tunnel Experiments on Single Degree of Freedom Flutter of Ailerons in the Hige Subsonic Speed Range. NACA TN 3687.

[6] Robert F. Thompson: Investigation of a 42.7° Sweptback Wing Model to Determine the Effects of Trailing-Edge Thickness on the Aileron Hinge Moment and Flutter Characteristics at Transonic Speeds. NACA RM L50J06.

[7] Erickson, Albtert L., and Stephenson, Jack D: A Suggested Method of Analyzing for Transonic Flutter of Control Surfaces Based on Available Experimental Evidence. NACA RM A7F30.

[8] William H. Phillips and James J. Adams: Low Speed Tests of a Model Simulating the Phenomenon of Control Surface Buzz. NACA RM L50F19.

[9] Albert L. Erickson and Robert C. Robinson: Some Preliminary Results in the Determination of Aerodynamic Derivatives of Control Surfaces in the Transonic Speed Range by Means of a Flush Type Electrical Pressure Cell. NACA RM A8H03.

[10] G. V. Bell, L. R. Fowell and D. H. Henshaw: The Interaction of Two Similarly Facing Shock Waves. UTIA Report No. 25.

[11] C. N. H. Lock and J. A. Beavan: Tunnel Interference at Compressibility Speeds Using the Flexible Walls of the Rectangular High Speed Tunnel. R & M 2005.

[12] Bernhard Goethert: Comments on Aileron Oscillations in the Shock Wave Range. AAF TR No. F-TR2101-ND, Materiel Command, Army Air Forces.